Title

A 3D model of human skeletal muscle innervated with stem cell-derived motor neurons enables epsilon-subunit targeted myasthenic syndrome studies

Authors

Mohsen Afshar Bakooshli[1,2], Ethan S Lippmann[3-5], Ben Mulcahy[6], Kayee Tung[7], Elena Pegoraro[8], Henry Ahn[7], Howard Ginsberg[1,7,9], Mei Zhen[6,10,11], Randolph S Ashton[3,4], Penney M Gilbert[1,2,12]*

Affiliations

[1]Institute of Biomaterials and Biomedical Engineering, University of Toronto, Toronto, ON, Canada

[2]Donnelly Centre for Cellular and Biomolecular Research, Toronto, ON, Canada

[3]Department of Biomedical Engineering, University of Wisconsin, Madison, WI, USA

[4]Wisconsin Institute for Discovery, University of Wisconsin, Madison, WI, USA

[5]Current address: Department of Chemical and Biomolecular Engineering, Vanderbilt University, Nashville, TN, USA

[6]Lunenfeld-Tanenbaum Research Institute, Mount Sinai Hospital, Toronto, ON, Canada

[7] Department of Surgery, University of Toronto, Toronto, ON, Canada

[8]Department of Neuroscience, University of Padova, Padova, Italy

[9]Li Ka Shing Knowledge Institute, Saint Michael's Hospital, Toronto, ON, Canada

[10]Department of Molecular Genetics, University of Toronto, Toronto, ON, Canada

[11]Department of Physiology, University of Toronto, Toronto, ON, Canada

[12] Department of Biochemistry, University of Toronto, Toronto, ON, Canada

Corresponding author: Penney M Gilbert

Correspondence should be addressed to:

Penney M. Gilbert

164 College Street

Rosebrugh Building, Rm. 407

Toronto, Ontario M5S3E1

Email: penney.gilbert@utoronto.ca

Ph: (416) 978-2501

Summary

Two-dimensional (2D) human skeletal muscle fiber cultures are ill equipped to support the contractile properties of maturing muscle fibers. This limits their application to the study of adult human neuromuscular junction (NMJ) development, a process requiring maturation of muscle fibers in the presence of motor neuron endplates. Here we describe a three-dimensional (3D) co-culture method whereby human muscle progenitors mixed with human pluripotent stem cell-derived motor neurons self-organize to form numerous functional NMJ connections within two weeks. Functional connectivity between motor neuron endplates and muscle fibers is confirmed with calcium transient imaging and electrophysiological recordings. Notably, we find epsilon acetylcholine receptor subunit protein expression and activity in our 3D co-culture demonstrating that the system supports a developmental shift from the embryonic to adult form of the receptor not previously reported in 2D culture. Further, co-culture treatment with myasthenia gravis patient sera demonstrates the ease of human disease studies using the system. This work provides the first method to model and evaluate adult NMJ development and disease in culture.

Introduction

The neuromuscular junction (NMJ) is a highly organized synapse formed between a motor neuron (MN) axon and a skeletal muscle fiber. It is designed to transmit efferent signals from projecting MNs to muscle fibers in order to actuate fiber contraction. Nicotinic acetylcholine receptors (AChRs) clustered at the NMJ's postsynaptic muscle fiber membrane mediate this signal by binding acetylcholine (ACh) neurotransmitters released from vesicles at the presynaptic MN axon terminal. AChRs are ligand-gated ion channels composed of five protein subunits. During development the gamma subunit in embryonic AChRs is replaced by an epsilon subunit in the adult synapse (Mishina et al., 1986; Missias et al., 1996). Previous animal studies showed that this AChR subunit transition occurs in the presence of motor axon endplates and confirmed that transcription of the epsilon gene (CHRNE) is stimulated by AChR Inducing Activity (ARIA) via ErbB receptors, a ligand of the neuregulin-1 (NRG1) family (Martinou et al., 1991) that is nerve derived. Consistently, CHRNE transcripts are detected in rodent 2D and 3D skeletal muscle fiber cultures when co-cultured with nerve cells (Bach et al., 2003; Ostrovidov et al., 2017; Smith et al., 2016; Vilmont et al., 2016). However, despite significant progress toward directing human pluripotent stem cells (PSCs) to the motor neuron lineage (Ashton et al., 2015; Hu and Zhang, 2010; Lippmann et al., 2014; Zhang et al., 2001) and establishing electrically and chemically responsive human muscle fibers in vitro (Madden et al., 2015), the first reports of human NMJ models – 2D human muscle fiber and motor neuron co-cultures – were unable to demonstrate synapse maturation via the gamma to epsilon AChR subunit switch (Guo et al., 2011; Steinbeck et al., 2016), and there are no reports of epsilon AChR protein expression or function in culture.

Congenital myasthenic syndrome is one of the most prevalent genetic diseases of the NMJ and commonly arises from mutations in one of the AChR encoding genes (Engel et al., 2010). The vast majority of mutations causing the disease arise in the CHRNE gene, the adult specific subunit of the AChR (Abicht et al., 2012; Engel et al., 1993). Given the lack of effective therapies for a wide range of neuromuscular diseases impacting the adult NMJ (Ohno et al., 1999), and that the majority of AChR mutations are mutations of the CHRNE (Ohno et al., 1995), a robust method to model the adult human NMJ in a dish is needed to synergize with recent advances in differentiating patient-derived PSCs to the MN lineage (Chen et al., 2011; Hu et al., 2010; Sances et al., 2016).

Here we report a method integrating architectural cues with co-culture techniques to create an environment conducive to formation of the adult human NMJ in as early as two weeks. We show that a 3D culture system is essential for long-term maintenance of maturing muscle fibers in culture. It supports the formation of AChR clusters primed for synaptogenesis and transition from the embryonic to the adult NMJ composition upon contact with MN endplates. We demonstrate that trophic factors produced by MNs induce AChR clustering and maturation in 3D muscle fiber cultures. We confirm formation of functional NMJ connections by imaging muscle fiber calcium transients and capturing electrophysiological recordings in response to glutamate-induced MN firing. We show that the 3D co-culture platform, and not 2D culture systems, supports the transition from the embryonic to the adult AChR, thereby enabling the functional assessment of the adult neuromuscular junction in vitro. Finally, we demonstrate the versatility and ease of our system for modelling human disease by treating neuromuscular co-cultures with IgG purified from myasthenia gravis (MG) patient sera together with human complement which resulted in readily visible clinical phenotypes in as early as two weeks culture

time. Thus, the described 3D co-culture model enables investigation of the adult human NMJ and therefore adult forms of neuromuscular diseases in vitro for the first time.

Results

Myogenic differentiation in 3D enhances fiber maturation and AChR clustering

We performed a side-by-side comparison of human skeletal muscle fiber populations derived in standard 2D culture versus 3D culture and uncovered differences in fiber maturation and AChR clustering. We established primary myogenic progenitor and fibroblast-like cell lines from human biopsy tissues (Blau and Webster, 1981) (**Figure S1A**), and seeded them at defined ratios either within a fibrin/Geltrex™ hydrogel (3D) or into 12-well tissue culture plastic dishes coated with Geltrex™ (2D) or a fibrinogen/Geltrex™ blend (2D; **Figure S1B**). Muscle cell laden hydrogels were formed within a polydimethylsiloxane channel and anchored at each end of the channel to the nylon hooks of Velcro™ fabrics, which act as artificial tendons and establish uniaxial tension during 3D tissue remodelling and differentiation (Bell et al., 1979; Madden et al., 2015; Vandenburgh et al., 1988) (**Figures S1C-D**).

Immunofluorescence analysis of the muscle contractile protein sarcomeric α-actinin (SAA) revealed the uniform alignment of striated muscle fibers along the tension axis in the 3D tissues (**Figure 1A, top panels** and **Figure S1E**), while 2D muscle fiber cultures were regionally aligned (**Figure 1A, bottom panels**), but globally disorganized (**Figure S1F).** In contrast to the muscle fibers established in 2D cultures, those derived in 3D culture progressively increased in diameter over three weeks in culture (**Figure 1B**) while maintaining fiber alignment and assembled contractile apparatus. Furthermore, over time in 3D culture, muscle tissues upregulated expression of the fast and slow adult isoforms of myosin heavy chain (MHC), which was accompanied by a downregulation of embryonic MHC expression, suggesting a gradual sarcomere structural maturation (**Figure 1C**). The absence of these trends in 2D muscle fiber culture may be explained by the inability of tissue culture plastic to support muscle fiber

contraction resulting in the increased incidence of damaged fibers observed in 2D (**Figure S1F, right panel)** and an enrichment of small, immature fibers (**Figures S1G-H**).

In support of our molecular characterization, 3D human muscle tissues were capable of generating active force in just 10 days of differentiation as evidenced by spontaneous twitches (**Movie S1**), which were not observed in 2D cultures. Consistent with prior reports (Madden et al., 2015), two-week old 3D muscle tissue twitch response could be paced by low frequency electrical stimuli (1Hz; **Movie S1**), which converted into tetanus contractions in response to increased frequency (20Hz; **Movie S1**). Similarly, ACh stimulation (10 μM) produced an immediate tetanus response (**Movie S1)** in 3D tissues suggesting an abundance of active AChRs, while the response of 2D muscle fiber cultures at this time-point was significantly less and inevitably led to the damage of the muscle fibers (**Movie S2**).

To evaluate the calcium handling capacity of 3D muscle fiber cultures, we transduced human muscle progenitor cells with lentiviral particles encoding GCaMP6 (Chen et al., 2013), a sensitive calcium indicator protein, driven by the MHCK7 (Madden et al., 2015) promoter, a muscle specific gene. Muscle fibers in 3D tissues generated strong collective calcium transient in response to electrical stimulation and immediately following exposure to ACh (**Figures S2A-C** and **Movie S3)**.

To evaluate the electrophysiological characteristics of single muscle fibers in 3D cultures, muscle progenitor cells were stably transduced with a light-gated ion channel, channelrhodopsin-2 (ChR2), driven by an EF1α promoter (Zhang et al., 2007). 3D muscle tissues generated using optogenetically-responsive muscle progenitor cells contracted in response to light stimulation on the second week of the culture (**Movie S4**). Next, single muscle fiber membrane potentials were

recorded using sharp microelectrode recording (**Figure S2D**) and light activation generated a clear depolarization of the membrane potential (**Figure S2E**).

Finally, we compared AChR clustering, an integral step in NMJ development, in 2D and 3D muscle fiber cultures. Both the number and size of AChR clusters was significantly greater in 3D muscle tissues (**Figure 1D**). In addition, over time in culture AChRs in 3D tissues transformed from oval-like patterns into multi-perforated clusters with pretzel-like shapes (**Figure 1E**).

Overall our comparison of muscle fibers established in 2D and 3D formats suggests that a 3D culture method is ideal to support rapid contractile apparatus maturation and function, as well as AChR clustering and function.

3D human neuromuscular co-cultures recapitulate early NMJ synaptogenesis

Since muscle fiber maturation is a prerequisite for NMJ development (Fox, 2009), we evaluated the hypothesis that the 3D skeletal muscle tissue platform would be well suited for human PSC-derived MN incorporation to model human NMJ synaptogenesis. We utilized MN clusters (Day 20, **Figure S3A)** differentiated from WA09 human embryonic stem cell – derived $OLIG2^{+}$ progenitor cells (**Figure S3B**) (Lippmann et al., 2015). MN clusters were enriched for cells expressing the HB9 and ISL1 transcription factors as well as the mature neurofilament marker SMI32 (**Figure S3C**). MN clusters were collected prior to muscle tissue preparation, mixed with the muscle progenitor cells in the hydrogel mix and seeded together into the PDMS channels. The 3D skeletal muscle tissue media was optimized to support co-culture health by supplementation with brain derived and glial cell line derived neurotrophic factors (BDNF, GDNF) to support MN viability. Co-cultures examined after 10 days in differentiation media

showed close contact between the MN clusters and the muscle tissue by phase-contrast microscopy (**Figure 2A**). Immunostaining co-cultures on the second week of culture for SMI-32, sarcomeric α-actinin, and α-bungarotoxin (to visualize AChRs) revealed that the co-cultures self-organized such that muscle progenitor cells fused to form multinucleated, aligned and striated muscle fibers and the MN clusters were positioned at the periphery of muscle bundles (**Figure 2A**).

Remarkably, the MNs were capable of regrowing neurites that were found in contact with α-bungarotoxin positive AChR clusters on muscle fibers (**Figure 2A, middle and right panels**). In vivo studies by others found that postsynaptic AChR aggregation on muscle fibers is supported by agrin secretion from the growing end of MN axons (Gautam et al., 1996). PSC-derived MNs express agrin (**Figure 2B**) and western blot analysis of neuromuscular co-cultures confirmed expression of MuSK and rapsyn proteins, two decisive synaptic proteins for mediating agrin-induced synaptogenesis (Glass and Yancopoulos, 1997) (**Figure S3E-F**). Consistently, we observed more and larger α-bungarotoxin positive AChR clusters in 3D neuromuscular co-cultures (**Figures 2C** and **2D**), particularly at sites where MN neurites made contact with muscle fibers (**Figure 2A, middle panel**). By supplementing 3D human muscle tissue media with neural agrin (50 ng/mL) we phenocopied these co-culture results (**Figures 2C** and **2E**). An evaluation of 2D neuromuscular co-cultures at the same time-point revealed a local alignment of the neurites and muscle fibers (**Figure S3D**), and a qualitative improvement in muscle fiber number and integrity (data not shown). However, only rare muscle fibers had clustered AChRs and we could not detect co-localization of the AChRs with SMI-32 stained neurites (**Figure S3D**).

In further support of 3D muscle fiber synaptogenic maturation, the LAMB2 gene encoding for the laminin beta 2 chain was expressed by the 3D human muscle tissues and co-

cultures (**Figure 2F**), and the protein was found enriched at the AChR clusters (**Figure 2G**). This is consistent with prior reports demonstrating laminin beta 2 concentrated at the neuromuscular junction synaptic cleft (Hunter et al., 1989) and the involvement of this tissue restricted basement membrane protein in NMJ maturation (Noakes et al., 1995).

Our characterizations demonstrate that a 3D co-culture system, but not 2D co-cultures, recapitulates many aspects of early synaptogenesis that were first identified with in vivo studies. We also demonstrate the feasibility of carrying out standard biological assays with this system.

3D human neuromuscular co-cultures are functionally innervated

We next sought to evaluate NMJ functionality in our neuromuscular co-cultures. With a combination of calcium handling analyses and electrophysiological recordings we report that 3D human neuromuscular co-cultures are functionally innervated in as early as two weeks. Using the fluorescent styryl dye FM 1-43 (Gaffield and Betz, 2007) and confocal microscopy we performed exocytosis assays on differentiated MNs (day 20) and confirmed that human PSC-derived MNs exocytose in response to high potassium (60 mM) and the excitatory neurotransmitter, L-glutamate (50 μM) (**Figures S4A-B** and **Movie S5**). The latter is particularly important, since the amino acid glutamate is a neurotransmitter that specifically stimulates MN cells but not muscle fibers (50 μM; **Movie S3**).

Next, we stimulated neuromuscular co-cultures that were generated using GCaMP6 transduced muscle progenitor cells with a 50 μM glutamate solution and observed calcium transients in the muscle fibers in close proximity to the MN clusters in as early as 14 days of co-culture (**Figures 3A-B** and **Movie S6**), indicating the formation of functional connectivity between MN endplates and muscle fibers. ACh stimulation on the same tissues after glutamate

stimulation provided a rapid way to visualize all muscle fibers in the tissue and revealed that many, but not all fibers were functionally innervated (**Figures 3A, right panel** and **Movie S6**). In contrast, and as expected, we observed very few functional connections when evaluating 2D neuromuscular co-cultures matured for 2-weeks and then treated with glutamate (**Figure S4C** and **Movie S7**). Indeed, a prior report of 2D human neuromuscular co-cultures performed functional assays only after 60 days of culture (Steinbeck et al., 2016). To confirm that the muscle fibers were functional, 2D co-cultures were stimulated with ACh (100 μM). Recorded calcium transients indicated the presence of responsive muscle fibers in close proximity to the MN cluster (**Figure S4C, right panel** and **Movie S7**).

To determine the maximum length of the functional connectivity between the MN cluster and the muscle fibers, we generated 3D neuromuscular tissues using GCaMP6 transduced muscle progenitor cells and a single MN cluster. On the second week of the culture, calcium transients of the 3D neuromuscular tissues were recorded during glutamate (50 μM) stimulation. Analysis of pre- and post-stimulation movies indicated an average maximum functional connectivity length of 1042.7±104.5 μm (n=3) at this time-point and, as expected, the number of innervated fibers decreased as the distance from the MN cluster increased (**Figure 3C**).

Finally, we performed electrophysiological recording to directly address the functional properties of the neuromuscular junctions. Using current clamp, we observed spontaneous miniature endplate potentials (mEPPs) from single muscle fibers that were proximal to the MN cluster (**Figure 3D**), which was absent in muscle-alone cultures (**Figure S2E**). Upon glutamate stimulation, the frequency of mEPPs was increased (**Figure 3E**), whereas the amplitude of mEPP remained unchanged (**Figure 3F**). These results support the notion that the MNs were stimulated by glutamate to release neurotransmitter. Moreover, in these muscle fibers, we

observed a few events that resembled action potentials in response to glutamate stimulation (**Figure 3G**). These events were characterized by a ~26 mV depolarization followed by a small plateau phase lasting ~8.5-14.5 milliseconds, and the absence of an afterhyperpolarization.

Together, these studies indicate that 3D neuromuscular co-cultures support efficient functional innervation that occurs 4-fold faster than reported for 2D neuromuscular co-cultures (Steinbeck et al., 2016).

3D human neuromuscular co-cultures to model the adult NMJ

Next, given the high degree of innervation achieved in our neuromuscular co-cultures, we hypothesized that the 3D model might be capable of supporting the gamma (embryonic) to epsilon (adult)-subunit switch that was not observed in 2D human neuromuscular co-cultures (Steinbeck et al., 2016). Western blot experiments on PSC-derived MNs confirmed the expression of NRG1-β1 in our differentiated MNs that was absent from muscle cultures (**Figure S4D**). Next, we quantified expression of the CHRNE, in our 2D and 3D muscle and neuromuscular cultures. We observed a significant increase in the expression of the CHRNE gene in co-cultures compared to muscle-alone cultures, in both 2D and 3D, at two weeks of culture (**Figures S4E**), suggesting the involvement of MN derived trophic factors. Treating the 3D muscle-alone cultures with motor neuron-derived conditioned media did not increase epsilon subunit gene expression above what we observed for untreated 3D muscle alone cultures (CHRNE 0.5% ± 0.4 % of GAPDH expression), suggesting that MN axon contact with muscle fibers may serve a role in modulating epsilon gene expression in muscle fibers. To test whether the increase can be associated with NRG1-β1-mediated induction of the CHRNE gene, we supplemented our 2D and 3D muscle-alone cultures with recombinant NRG1- β1 (5 nM) and

detected a significant increase in CHRNE expression in the supplemented muscle fiber cultures (**Figure S4E**). However, when we evaluated AChR epsilon expression at the protein level, it was only upregulated in the 3D co-culture condition (**Figure 4A**) and not in 2D co-cultures (**Figure 4D**). The upregulation of AChR epsilon protein expression in 3D co-cultures was accompanied by a significant increase in AChR-beta (**Figure 4B**) and a relative decrease in the AChR gamma subunit (**Figure 4C**), further supporting the gamma-to-epsilon switch in 3D co-cultures. Notably, we did not observe similar MN-dependent changes in the protein levels of AChR subunits (beta, gamma, and epsilon) in 2D co-cultures (**Figure 4D**).

We next sought to determine if the 3D human neuromuscular co-culture system was suitable for modelling congenital myasthenic syndromes caused by mutations in CHRNE by blocking the AChR-epsilon subunit using WTX; a peptide that selectively binds and blocks the epsilon subunit of the muscle AChR (McArdle et al., 1999). 3D neuromuscular tissues were generated using GCaMP6 transduced muscle progenitor cells, and each tissue was stimulated with glutamate twice, pre- and post WTX treatment (1 μM), with a 24-hour recovery time allocated between each stimulation. Co-culture movies recorded during glutamate stimulation were then analyzed for the area of the reactive muscle fibers post glutamate stimulation using GCaMP6 fluorescence signal pre- and post-WTX treatment at defined regions of interests (**Figure 4E** and **Movie S8**). Quantification showed a 46.47 ± 15% (n=3; $P<0.05$) decrease in the area of reactive muscle fibers in response to glutamate stimulation in WTX treated neuromuscular tissues (**Figure 4E-F**). Notably, we did not detect a significant change in muscle fiber calcium transients of in our 2D neuromuscular co-cultures following glutamate stimulation pre- and post-WTX treatment (**Movie S7**), nor did we observe it in 3D muscle cultures alone treated with WTX and stimulated with ACh **(Movie S9)**. This data suggests that a 3D

neuromuscular co-culture platform is required to rapidly and easily model and study diseases impacting the adult NMJ.

To demonstrate the tractability and robustness of the 3D neuromuscular co-culture system to model autoimmune myasthenia gravis, we treated co-culture tissues with IgG isolated from 3 patients afflicted with AChR-targeted myasthenia gravis (**Table S4**). IgG from a healthy patient serum served as the control. Myasthenia gravis (MG) is an autoimmune disease manifesting as muscle weakness caused by the production of autoantibodies that alter, block, or destroy NMJ receptors required for signal transmission. Previous studies have shown the involvement of the complement system in the pathogenesis of patients diagnosed with AChR-targeted MG (Engel and Fumagalli, 1982; Steinbeck et al., 2016). IgG and complement deposit at the NMJ causing inflammation and destruction of the AChRs on the postsynaptic NMJ membrane (Engel et al., 1977). Therefore, we treated our neuromuscular tissues with healthy and MG patient IgG (300 nM) as well as human serum containing complement. Localized deposition of complement on BTX stained AChRs was confirmed by staining for the complement C3c one-day following treatment of muscle tissues with MG IgG and active human complement (**Figure 4G**). As expected, we observed smaller AChR clusters on muscle fibers of tissues treated with MG IgG compared to control IgG (**Figure 4H-I**). Furthermore, 3 days after IgG and human complement treatment, the area of reactive muscle fibers was quantified from short videos capturing GCaMP6 signals after neurotransmitter stimulation. The results revealed a significant decrease in the area of the reactive muscle fibers after ACh (**Figure 4J**, **Figure S4F** and **Movie S10**) and glutamate stimulation in the MG samples as compared to the controls (**Figure 4K-L** and **Movie S11**).

Discussion

Here we report the first method to co-culture 3D human skeletal muscle fiber tissues together with human PSC-derived MNs. We demonstrate that functional innervation is achieved in 3D, but not 2D neuromuscular co-cultures within 2-weeks of culture. Indeed, we find that innervation in 3D neuromuscular co-cultures is ~4-fold faster and more efficient than a prior report of a 2D human neuromuscular co-culture system (Steinbeck et al., 2016), and we show that this simplifies studies of myasthenia gravis in a dish. With side-by-side comparisons of 2D and 3D muscle-alone and neuromuscular co-cultures, we confirmed that CHRNE transcription is supported by innervation in 2D and 3D, and then show that the AChR epsilon subunit protein is only functionally integrated into the AChR in the context of 3D neuromuscular co-cultures. Therefore, this is the first report of a culture method to study the AChR gamma to epsilon subunit developmental switch in culture and to model diseases of the adult human NMJ in a dish.

Our side-by-side comparison of human skeletal muscle fiber cultures in 2D and 3D indicates the structural and functional advantages of a 3D culture model over 2D systems. The value of 3D culture is reported in previous studies for other organs (Lancaster and Knoblich, 2014), and in this study we provide the first evidence that 3D culture conditions are indispensable for maturation of multinucleated muscle fibers due to their capability to accommodate the inherent contractile nature of the muscle fibers in the long-term. This in turn leads to muscle fiber hypertrophy, improved calcium handling, and muscle fiber maturation as evidenced by expression of adult forms of MHC, and elaborated clustering of AChRs. This makes 3D neuromuscular cultures an ideal platform for studying NMJ synaptogenesis given the innately long process required for functional NMJ development to occur.

Consistently, electrophysiological recordings of single muscle fibers in these neuromuscular co-cultures detected spontaneous and stimulated mEPPs, suggesting that MNs form functional neuromuscular junctions, similar to that observed in in vivo mammalian models. The properties of observed action potentials in these cultures is consistent with the possibility that the 3D human neuromuscular cultures are not fully mature – an observation that concurs with the relatively small muscle fibers – and indicating additional chemical or physical cues are necessary to mature the tissues further. We anticipate that increasing culture times, electrical stimulation, and / or addition of trophic or synaptogenesis factors might improve the maturity of the neuromuscular culture and their connections.

Perhaps most strikingly, 3D neuromuscular cultures robustly produce functional adult AChR epsilon subunit, which is, to our knowledge, the first report of a system that supports the gamma to epsilon AChR subunit switch in culture. This, we hypothesize, is induced in response to NRG1 secreted from MN axons in co-cultures with mature muscle fibers in 3D. In a proof-of-concept study, we demonstrate the application of our NMJ model to study adult NMJ activity by using a peptide that specifically blocks the epsilon subunit. Treatment with the peptide dampened glutamate-induced GCaMP6 calcium reporter activity in neuromuscular co-cultures demonstrating the utility of the system for adult NMJ studies. While we observed CHRNE transcript expression upregulated in 2D neuromuscular co-cultures, we did not observe the protein and function (WTX-responsivity) level changes we detected in 3D neuromuscular cultures. This suggests the intriguing possibility that the epsilon subunit of the AChR is subjected to post-translational modifications and/or intracellular trafficking events that are only supported in the 3D neuromuscular co-cultures.

In summary, our method to model the adult human NMJ in a dish provides a versatile approach to study skeletal muscle and NMJ development, but more importantly, provides the first reproducible method to study adult, rather than embryonic, NMJ activity in as early as two weeks of co-culture time. Our calcium reporter neuromuscular tissues can easily be integrated with other optogenetic methods (Steinbeck et al., 2016) to further elucidate synaptic transmission mechanisms in adult NMJ, such as adult AChR conductance. Furthermore, neuromuscular co-cultures may be integrated with other neuron populations such as upper MNs and / or myelinating Schwann cells to support studies aimed at a better understanding of signal transmission in the central nervous system. The method now enables modelling diseases that target the adult NMJ (e.g. congenital myasthenia gravis) as well as MN dependent disorders of the NMJ (e.g. spinal muscular atrophy and amyotrophic lateral sclerosis). Finally, the 3D human NMJ system can serve as an improved pre-clinical pharmacological testing platform to evaluate drugs designed for NMJ disorders or to support personalized medicine applications.

References

Abicht, A., Dusl, M., Gallenmüller, C., Guergueltcheva, V., Schara, U., Della Marina, A., Wibbeler, E., Almaras, S., Mihaylova, V., von der Hagen, M., et al. (2012). Congenital myasthenic syndromes: Achievements and limitations of phenotype-guided gene-after-gene sequencing in diagnostic practice: A study of 680 patients. Hum. Mutat. *33*, 1474–1484.

Ashton, R., Lippmann, E., Estevez-Silva, M., and Ashton, R. (2015). Chemically defined differentiation of human pluripotent stem cells to hindbrain and spinal cord neural stem cells with defined regional identities. Protoc. Exch.

Bach, A.D., Beier, J.P., and Stark, G.B. (2003). Expression of Trisk 51, agrin and nicotinic-acetycholine receptor epsilon-subunit during muscle development in a novel three-dimensional muscle-neuronal co-culture system. Cell Tissue Res. *314*, 263–274.

Bell, E., Ivarsson, B., and Merrill, C. (1979). Production of a tissue-like structure by contraction of collagen lattices by human fibroblasts of different proliferative potential in vitro. Proc. Natl. Acad. Sci. U. S. A. *76*, 1274–1278.

Blau, H.M., and Webster, C. (1981). Isolation and characterization of human muscle cells. Proc. Natl. Acad. Sci. *78*, 5623–5627.

Chen, G., Gulbranson, D.R., Hou, Z., Bolin, J.M., Ruotti, V., Probasco, M.D., Smuga-Otto, K., Howden, S.E., Diol, N.R., Propson, N.E., et al. (2011). Chemically defined conditions for human iPSC derivation and culture. Nat. Methods *8*, 424–429.

Chen, T.-W., Wardill, T.J., Sun, Y., Pulver, S.R., Renninger, S.L., Baohan, A., Schreiter, E.R., Kerr, R.A., Orger, M.B., Jayaraman, V., et al. (2013). Ultrasensitive fluorescent proteins for imaging neuronal activity. Nature *499*, 295–300.

Engel, A.G., and Fumagalli, G. (1982). Mechanisms of acetylcholine receptor loss from the neuromuscular junction. Ciba Found. Symp. 197–224.

Engel, A.G., Lambert, E.H., and Howard, F.M. (1977). Immune complexes (IgG and C3) at the motor end-plate in myasthenia gravis: ultrastructural and light microscopic localization and electrophysiologic correlations. Mayo Clin. Proc. *52*, 267–280.

Engel, A.G., Hutchinson, D.O., Nakano, S., Murphy, L., Griggs, R.C., Gu, Y., Hall, Z.W., and Lindstrom, J. (1993). Myasthenic syndromes attributed to mutations affecting the epsilon subunit of the acetylcholine receptor. Ann. N. Y. Acad. Sci. *681*, 496–508.

Engel, A.G., Shen, X.-M., Selcen, D., and Sine, S.M. (2010). What Have We Learned from the Congenital Myasthenic Syndromes. J. Mol. Neurosci. *40*, 143–153.

Fox, M.A. (2009). Development of the Vertebrate Neuromuscular Junction. In The Sticky Synapse, H. Umemori, and M. Hortsch, eds. (Springer New York), pp. 39–84.

Gaffield, M.A., and Betz, W.J. (2007). Imaging synaptic vesicle exocytosis and endocytosis with FM dyes. Nat. Protoc. *1*, 2916–2921.

Gautam, M., Noakes, P.G., Moscoso, L., Rupp, F., Scheller, R.H., Merlie, J.P., and Sanes, J.R. (1996). Defective Neuromuscular Synaptogenesis in Agrin-Deficient Mutant Mice. Cell *85*, 525–535.

Glass, D.J., and Yancopoulos, G.D. (1997). Sequential roles of agrin, MuSK and rapsyn during neuromuscular junction formation. Curr. Opin. Neurobiol. *7*, 379–384.

Guo, X., Gonzalez, M., Stancescu, M., Vandenburgh, H.H., and Hickman, J.J. (2011). Neuromuscular junction formation between human stem cell-derived motoneurons and human skeletal muscle in a defined system. Biomaterials *32*, 9602–9611.

Hu, B.-Y., and Zhang, S.-C. (2010). Directed differentiation of neural-stem cells and subtype-specific neurons from hESCs. Methods Mol. Biol. Clifton NJ *636*, 123–137.

Hu, B.-Y., Weick, J.P., Yu, J., Ma, L.-X., Zhang, X.-Q., Thomson, J.A., and Zhang, S.-C. (2010). Neural differentiation of human induced pluripotent stem cells follows developmental principles but with variable potency. Proc. Natl. Acad. Sci. *107*, 4335–4340.

Hunter, D.D., Shah, V., Merlie, J.P., and Sanes, J.R. (1989). A laminin-like adhesive protein concentrated in the synaptic cleft of the neuromuscular junction. Nature *338*, 229.

Lancaster, M.A., and Knoblich, J.A. (2014). Organogenesis in a dish: Modeling development and disease using organoid technologies. Science *345*, 1247125.

Lippmann, E.S., Estevez-Silva, M.C., and Ashton, R.S. (2014). Defined Human Pluripotent Stem Cell Culture Enables Highly Efficient Neuroepithelium Derivation Without Small Molecule Inhibitors. STEM CELLS *32*, 1032–1042.

Lippmann, E.S., Williams, C.E., Ruhl, D.A., Estevez-Silva, M.C., Chapman, E.R., Coon, J.J., and Ashton, R.S. (2015). Deterministic HOX Patterning in Human Pluripotent Stem Cell-Derived Neuroectoderm. Stem Cell Rep. *4*, 632–644.

Madden, L., Juhas, M., Kraus, W.E., Truskey, G.A., and Bursac, N. (2015). Bioengineered human myobundles mimic clinical responses of skeletal muscle to drugs. ELife e04885.

Mamchaoui, K., Trollet, C., Bigot, A., Negroni, E., Chaouch, S., Wolff, A., Kandalla, P.K., Marie, S., Di Santo, J., St Guily, J.L., et al. (2011). Immortalized pathological human myoblasts: towards a universal tool for the study of neuromuscular disorders. Skelet. Muscle *1*, 34.

Martinou, J.C., Falls, D.L., Fischbach, G.D., and Merlie, J.P. (1991). Acetylcholine receptor-inducing activity stimulates expression of the epsilon-subunit gene of the muscle acetylcholine receptor. Proc. Natl. Acad. Sci. U. S. A. *88*, 7669–7673.

McArdle, J.J., Lentz, T.L., Witzemann, V., Schwarz, H., Weinstein, S.A., and Schmidt, J.J. (1999). Waglerin-1 Selectively Blocks the Epsilon Form of the Muscle Nicotinic Acetylcholine Receptor. J. Pharmacol. Exp. Ther. *289*, 543–550.

Mishina, M., Takai, T., Imoto, K., Noda, M., Takahashi, T., Numa, S., Methfessel, C., and Sakmann, B. (1986). Molecular distinction between fetal and adult forms of muscle acetylcholine receptor. Nature *321*, 406–411.

Missias, A.C., Chu, G.C., Klocke, B.J., Sanes, J.R., and Merlie, J.P. (1996). Maturation of the acetylcholine receptor in skeletal muscle: regulation of the AChR gamma-to-epsilon switch. Dev. Biol. *179*, 223–238.

Noakes, P.G., Gautam, M., Mudd, J., Sanes, J.R., and Merlie, J.P. (1995). Aberrant differentiation of neuromuscular junctions in mice lacking s-laminin/laminin β2. Nature *374*, 258.

Ohno, K., Hutchinson, D.O., Milone, M., Brengman, J.M., Bouzat, C., Sine, S.M., and Engel, A.G. (1995). Congenital myasthenic syndrome caused by prolonged acetylcholine receptor channel openings due to a mutation in the M2 domain of the epsilon subunit. Proc. Natl. Acad. Sci. U. S. A. *92*, 758–762.

Ohno, K., Anlar, B., and Engel, A.G. (1999). Congenital myasthenic syndrome caused by a mutation in the Ets-binding site of the promoter region of the acetylcholine receptor epsilon subunit gene. Neuromuscul. Disord. NMD *9*, 131–135.

Ostrovidov, S., Ahadian, S., Ramon-Azcon, J., Hosseini, V., Fujie, T., Parthiban, S.P., Shiku, H., Matsue, T., Kaji, H., Ramalingam, M., et al. (2017). Three-dimensional co-culture of C2C12/PC12 cells improves skeletal muscle tissue formation and function. J. Tissue Eng. Regen. Med. *11*, 582–595.

Sances, S., Bruijn, L.I., Chandran, S., Eggan, K., Ho, R., Klim, J.R., Livesey, M.R., Lowry, E., Macklis, J.D., Rushton, D., et al. (2016). Modeling ALS with motor neurons derived from human induced pluripotent stem cells. Nat. Neurosci. *16*, 542–553.

Smith, A.S.T., Passey, S.L., Martin, N.R.W., Player, D.J., Mudera, V., Greensmith, L., and Lewis, M.P. (2016). Creating Interactions between Tissue-Engineered Skeletal Muscle and the Peripheral Nervous System. Cells Tissues Organs *202*, 143–158.

Steinbeck, J.A., Jaiswal, M.K., Calder, E.L., Kishinevsky, S., Weishaupt, A., Toyka, K.V., Goldstein, P.A., and Studer, L. (2016). Functional Connectivity under Optogenetic Control Allows Modeling of Human Neuromuscular Disease. Cell Stem Cell *18*, 134–143.

Vandenburgh, H.H., Karlisch, P., and Farr, L. (1988). Maintenance of highly contractile tissue-cultured avian skeletal myotubes in collagen gel. In Vitro Cell. Dev. Biol. *24*, 166–174.

Vilmont, V., Cadot, B., Ouanounou, G., and Gomes, E.R. (2016). A system for studying mechanisms of neuromuscular junction development and maintenance. Development *143*, 2464–2477.

Zhang, F., Wang, L.-P., Brauner, M., Liewald, J.F., Kay, K., Watzke, N., Wood, P.G., Bamberg, E., Nagel, G., Gottschalk, A., et al. (2007). Multimodal fast optical interrogation of neural circuitry. Nature *446*, 633–639.

Zhang, S.C., Wernig, M., Duncan, I.D., Brüstle, O., and Thomson, J.A. (2001). In vitro differentiation of transplantable neural precursors from human embryonic stem cells. Nat. Biotechnol. *19*, 1129–1133.

Experimental Procedures

Human skeletal muscle cell isolation and culture

Human skeletal muscle tissues removed in the course of scheduled surgical procedures and designated for disposal were utilized in this study in accordance with St. Michael's Hospital research ethics board and University of Toronto administrative ethics review approval. Small skeletal muscle samples (~1 cm^3) were taken from the multifudus muscle of patients undergoing lumbar spine surgery. Primary myoblast and fibroblast-like cell lines were established and maintained as previously described (Blau and Webster, 1981). Briefly, human skeletal muscle samples were minced and then dissociated into a single cell slurry with clostridium histolyticum collagenase (Sigma, 630 U/mL) and dispase (Roche, 0.03 U/mL) in Dulbecco's Modified Eagle's medium (DMEM; Gibco). The cell suspension was passed multiple times through a 20 G needle to facilitate the release of the mononucleated cell population and subsequently depleted of red blood cells with a brief incubation in red blood cell lysis buffer (**Table S2**). The resulting cell suspension containing a mixed population of myoblasts and fibroblast-like cells was plated in a collagen-coated tissue culture dish containing myoblast growth medium: F-10 media (Life Technologies), 20% fetal bovine serum (Gibco), 5 ng/mL basic fibroblast growth factor (bFGF; ImmunoTools) and 1% penicillin-streptomycin (Life Technologies). After one passage, the cell culture mixture was stained with an antibody recognizing the neural cell adhesion molecule (NCAM/CD56; BD Pharmingen), and the myogenic progenitor ($CD56^+$) and fibroblast-like cell ($CD56^-$) populations were separated and purified using fluorescence-activated cell sorting (FACS). Subsequent experiments utilized low passage cultures (P4—P9).

Two-dimensional culture of human skeletal muscle cells

Human primary muscle progenitor cells were mixed with primary muscle fibroblast-like cells at the following ratios: CD56+ (95%) and CD56^{-} (5%). $3x10^6$ cells in myoblast growth media lacking bFGF were plated into each well of a Geltrex™ (Life Technologies) coated 12-well multi-well plate. For Geltrex™ culture dish coating, 1 mg of Geltrex™ was resuspended in 12 mL of cold DMEM and transferred to wells of a 12 well plate (1 mL per well). Plates were left in a 37 °C incubator overnight. On the following day, media was aspirated prior to cell culture. The culture media was exchanged 2 days later with myoblast differentiation media. Half of the culture media was exchanged every other day thereafter. In some experiments fibrinogen was supplemented in the differentiation media at 10 μg/mL during the differentiation phase to control for the effect of fibrinogen receptor ligation on two-dimensional (2D) muscle fiber differentiation.

Generation of three-dimensional human skeletal muscle tissues

Three-dimensional (3D) skeletal muscle tissues were generated in culture as previously described (Madden et al., 2015) with the following modification: FACS-purified myoblast and fibroblast-like cells were incorporated into tissues at established ratios as follows. CD56+ (95%) and CD56^{-} (5%) cells were resuspended in the hydrogel mixture (**Table S2**) in the absence of thrombin. Thrombin (Sigma) was added at 0.2 unit per mg of fibrinogen just prior to seeding the cell/hydrogel suspension into a custom-made device designed to impose uniaxial tension and then incubated for 5 minutes at 37°C to expedite fibrin polymerization. Myoblast growth media (**Table S2**) lacking bFGF but containing 1.5 mg/mL 6-aminocaproic acid (ACA; Sigma) was added. The culture media was exchanged 2 days later to myoblast differentiation medium (**Table S2**) containing 2 mg/mL ACA. Half of the culture media was exchanged every other day

thereafter. For agrin-induced AChR clustering experiments, recombinant rat agrin (R&D Systems) was supplemented in the culture media at 50 ng/ml over the course of the differentiation time. For Neuregulin-1-beta1 (NRG1-β1) induced AChR epsilon gene expression experiments, recombinant human NRG1-beta1 (R&D Systems) was supplemented in the culture media at 5 nM throughout the 2-week differentiation period.

Differentiation of human embryonic stem cells to post-mitotic motor neurons

Motor neurons were specified from WA09 hESCs (passage 25-45) as previously described (Lippmann et al., 2014, 2015). Briefly, hESCs were maintained on Matrigel (BD Biosciences) in E8 medium with insulin added at a concentration of 2 mg/L. For differentiation, hESCs were dissociated with accutase (Life Technologies) and reseeded at $1x10^5$ cells/cm^2 in E8 medium containing 10 μM ROCK inhibitor (Y27632; R&D Systems) in 6-well polystyrene tissue culture plates coated with 100 μg/mL poly-L-ornithine (PLO; Sigma) and 8 μg/well VTN-NC (gift from Dr. James Thomson). hESC were differentiated to $OLIG2^+$ progenitors in E6 medium containing the same insulin concentration as E8 medium as previously described (Lippmann et al., 2015). For differentiation of the $OLIG2^+$ progenitors to motor neurons, cells were sub-cultured by en bloc passage, reseeded at a 1:200 ratio in Geltrex™-coated 6-well plates, and differentiated for 14 days in E6 medium containing 1 μM retinoic acid (Sigma), 100 nM purmorphamine (Tocris), and 100 ng/mL sonic hedgehog (R&D systems). To facilitate neuronal maturation prior to myoblast co-culture, 5 μM DAPT (Tocris) was added from days 8-14.

Two- and three-dimensional human motor neuron cluster and skeletal muscle fiber co-culture

2D muscle fiber cultures were prepared as described above. 24 hours post seeding the myogenic progenitor cells, motor neuron clusters were detached using a 1 ml pipette tip and transferred to the muscle cell culture plates at a ratio of 5 motor neuron clusters per well in myoblast media lacking bFGF, but containing 10 ng/ml brain derived neurotrophic factor (BDNF) and 10 ng/ml glial cell line derived neurotrophic factor (GDNF). Mid-sized clusters (150 to 300 μm in diameter) were visually identified and selected for transfer. The culture media was replaced 24 hours later to myogenic differentiation media (**Table S2**) supplemented with 10 ng/mL BDNF and 10 ng/mL GDNF. Half of the culture media was exchanged every other day thereafter.

3D skeletal muscle tissue cell/hydrogel suspension was prepared as described above. Motor neuron clusters were transferred manually to the cell/hydrogel suspension at a ratio of 5 clusters per tissue. Thrombin was added and tissues were seeded as described above. Myoblast growth media lacking bFGF but containing 2 mg/mL 6-aminocaproic acid (ACA; Sigma), 10 ng/mL BDNF, and GDNF was added. The culture media was exchanged 2 days later to myogenic differentiation media (**Table S2)** and supplemented with 10 ng/mL BDNF and 10 ng/mL GDNF. Half of the culture media was exchanged every other day thereafter. 2D and 3D muscle cultures serving as neuromuscular co-culture controls were also supplemented with BDNF and GDNF. Co-cultures were analyzed at time points indicated in the figures and legends.

Immunostaining and fluorescence microscopy

All samples (2D cultures and 3D tissue whole mounts) were fixed in 4% PFA for 10 minutes and then washed with phosphate buffered saline (PBS). Following fixation, samples were incubated in blocking solution (**Table S2**) for at least 1 hour. Samples were incubated in primary antibody solutions diluted in blocking solution (**Table S1**) overnight at 4°C overnight. After several

washes in blocking solution, samples were incubated with appropriate secondary antibodies diluted in the blocking solution for 30 minutes at room temperature. Hoechst 33342/DRAQ5 (ThermoFisher) were used to counterstain cell nuclei. Images were acquired using an Olympus IX83 inverted confocal microscope with FV-10 software and analyzed using NIH ImageJ software.

Myofiber size analysis

Myofiber size was measured using 40X magnification images of the 2D cultures and 3D tissues at the indicated time points. Sarcomeric α-actinin stained confocal images of 2D muscle cultures and stack images of 3D muscle tissues were analyzed using NIH ImageJ software to quantify the diameter of each muscle fiber at the widest point.

Western blotting

3D tissues and 2D culture cell pellets were collected at the indicated time points, flash frozen in liquid nitrogen, and stored at -80 until all the time points were collected. Tissues and cell pellet samples were lysed in RIPA buffer (ThermoFisher) containing protease inhibitors, and then lysates were analyzed for total protein concentration using the BCA protein assay kit (ThermoFisher). 15 μg of protein, based on the BCA protein assay results, was analyzed. Western blot was performed using a Bio-Rad Power Pac 1000 and Trans-Blot Turbo Transfer System to transfer the proteins from a polyacrylamide gel to a nitrocellulose membrane. Primary antibodies **(Table S1)** were incubated with membranes over night at 4 °C in milk based blocking solution **(Table S2)**. Membranes were then washed 3 times each 30 minutes in a Tris-buffered saline with Tween (TBST; **Table S2**) and then transferred into blocking solution containing

horseradish peroxidase conjugated anti-rabbit and anti-mouse secondary antibodies (Cell Signaling; 1:5'000). Chemoluminescence was performed using ECL substrate (ThermoFisher). Images were analyzed using NIH ImageJ software.

AChR clustering assay

α-bungarotoxin staining was performed to visualize and measure the number and size of AChR clusters at different time points in 2D cell and 3D tissue cultures. Fixed tissues were incubated with 5 nM of Alexa Fluor 647 conjugated α-bungarotoxin for 30 minutes to label AChRs. Samples were washed and images were captured at 40X at a minimum of 6 random locations (0.1 mm^2 in area each). Images were analyzed using NIH ImageJ software. α-bungarotoxin-positive regions > 2 μm in length were classified as 'clusters' and analyzed.

Electrical stimulation

To ensure accurate and reproducible conditions for electrical stimulation, a custom made stimulation chamber was developed using a 35 mm petri-dish, 2 carbon rods, and platinum wires. The chamber was sterilized using 70% ethanol prior to experiments. Individual tissues were transferred to the chamber with differentiation media at day 14. Platinum wires were hooked up to a commercial function generator (Rigol DG1022U). A Rigol DS1102E digital oscilloscope was used to confirm the frequency and amplitude of the generated signal before connecting the pulse generator to the platinum wires. 3D tissues were stimulated with square pulses with 20% duty cycle, 5V amplitude (field strength of 1.67 V/cm), and the reported frequencies.

Calcium transient analysis

$CD56^+$ sorted human myogenic progenitor cells were transduced with a lentiviral vector encoding the fluorescent calcium indicator GCaMP6 driven by the muscle specific gene MHCK7 (generated by N.Bursac; AddGene plasmid #65042). Cells were then sorted to purify the infected cells based on GFP expression. 2D and 3D muscle tissues generated with human skeletal muscle progenitors expressing GCaMP6 were imaged using an Olympus IX83 microscope equipped with modules to control the temperature and CO_2 concentration. Movies were recorded under physiological condition (37 °C and 5% CO_2) in differentiation media using an Olympus DP80 dual CCD color and monochrome camera and CellSense™ software. Acetylcholine (BIO BASIC) was reconstituted to produce a 100 mM stock solution in PBS and was diluted to the final working concentration (as specified in the text) by addition directly into the chamber containing 2D or 3D muscle cultures. Waglerin-1 (Smartox Biotechnology) was prepared as a 100x stock solution in PBS and was added to the co-cultures to achieve a 1 μM working concentration 10 minutes before MN stimulation with glutamate. L-glutamate (Abcam) was first reconstituted to 100 mM in 1equal NaOH and then further diluted in HBSS (Gibco)/DMEM to produce the 100x stock solution (5 mM). Movies were analyzed using NIH ImageJ software.

To assess the effect of Waglerin-1 on glutamate-stimulated calcium transients, movies were projected into two 2D images for equal periods of time before and after glutamate stimulation. These 2D projected images were then subtracted to eliminate spontaneously active fibers from our analysis. Background from different imaging sessions were normalized and signals from GCaMP6 were analyzed to measure the area of reactive fibers post glutamate stimulation at the same ROIs before and after Waglerin-1 treatment.

Electrophysiological recordings

Individual muscle fibers were impaled with 30-40 MΩ sharp electrodes pulled from borosilicate glass (World Precision Instruments), filled with 3M KCl. Membrane potential was recorded in the current clamp configuration using a Digidata 1440A and MultiClamp 700 A amplifier (Axon Instruments, Molecular Devices). Data were digitized at 10 kHz and filtered at 2.6 kHz. Data were quantified using MiniAnalysis (Synaptosoft). Each fiber was allowed to recover for a few minutes, to allow its resting membrane potential to stabilize before recordings were performed. For electrophysiological recordings following optogenetic stimulation, 3D muscle tissues were generated using human skeletal muscle progenitors transduced with a lentiviral vector encoding humanized ChR2 with H134R mutation fused to EYFP driven by EF1a (generated by K. Deisseroth; AddGene plasmid #20942). Cells were sorted to purify the infected cells based on the EYFP signal. Optogenetic stimulation was performed using blue LED (KSL-70, RAPP OptoElectronic) using a wavelength of 470 nm, controlled by the Axon amplifier software. For glutamate addition, glutamate was pipetted by hand near the edge of the bath and allowed to diffuse to the tissue. For all recordings, the bath solution was standard DMEM (Gibco).

Alternative human skeletal muscle cell source

An alternative source of human myogenic progenitor cells was used in a subset of experiments (**Figures 4J-L, Figure S3D, Figure S4C** and **Figure S4F**). Immortalized myogenic progenitor cells were a gift from Dr. Vincent Mouly. Briefly, human-derived skeletal muscle cell (hSMC) lines were derived from healthy subjects. Immortalized hSMC were generated by transduction with human telomerase-expressing and cyclin-dependent kinase 4-expressing vectors, as previously described (Mamchaoui et al., 2011). Immortalized human myogenic progenitor cells were transduced lentivirally to express the fluorescent calcium indicator GCaMP6 as described

above. Cells were then sorted for GFP expression to enrich transduced cells and were further expanded in myoblast growth media (**Table S2**).

Myasthenia gravis disease modeling

Serum from 3 patients diagnosed with Anti-AChR MG (**Table S4**) was collected and IgG fractions were purified using a Protein A IgG purification kit (Thermofisher) based on the manufacturers manual. Purified IgG was reconstituted in phosphate buffer and the IgG content was measured using a nanodrop and was added to the differentiation culture media at 300 nM final concentration 3 days prior to glutamate stimulation on day 11 of co-culture. 2% human serum (Sigma) was supplemented together with the patient IgG in the differentiation medium rather than horse serum. IgG from healthy human serum (Sigma) was used as a control together with 2% human serum. Co-cultures were stimulated using glutamate and acetylcholine at indicated time points and calcium transients were captured by imaging the GCaMP6 signals using an Olympus IX83 microscope. Movies were then analyzed to measure the area of reactive fibers post glutamate and acetylcholine stimulation in MG and control IgG treated neuromuscular tissues as described above.

FM 1-43 labelling and imaging

Motor neuron clusters were separated from undifferentiated single cells using Accutase (ThermoFisher) and transferred to a Geltrex^{TM} coated 6-well plate on day 14 of differentiation. Clusters were then cultured for an additional week in E6 media supplemented with 10 ng/mL BDNF and 10 ng/mL GDNF to permit the regrowth of the neurites and were then labelled with the FM 1-43 styryl dye (Molecular Probes) following the manufacturer's manual. Briefly, MN

clusters were stimulated using high potassium solution (60 mM) and incubated with FM 1-43 (2 μM) in HBSS (+Mg^{2+} and +Ca^{2+}) for 20 minutes to allow the loading of the dye. Clusters were washed with HBSS for at least one hour at room temperature before imaging. Samples were imaged using an IX83 Olympus confocal microscope with FV-10 software at physiological conditions (37 °C and 5% CO_2). MN clusters were stimulated with either high potassium solution (60 mM in PBS) or L-glutamate (50 μM in HBSS) while acquiring time-lapse movie sequences. Movies were analysed for fluorescence intensity before and after stimulation using NIH ImageJ software.

Gene expression analysis

Total RNA was extracted from 3 consecutive co-culture samples using 3 biological replicates using the PureLink RNA Micro Kit according to the manufacturer's protocol (ThermoFisher). cDNA was reverse transcribed from 400 ng of RNA using the High-Capacity cDNA Reverse Transcription kit (Applied Biosystems). For quantitative real-time PCR (qRT-PCR), CHRNE and CHRNG primers were acquired from Bio-Rad and reactions were run according to manufacturer's protocol on the Roche LightCycler 480 (Roche) using LightCycler 480 SYBR Green I Master (Roche). All results are normalized to the housekeeping gene glyceraldehyde 3-phosphate dehydrogenase (GAPDH). Gene expression is reported in % of GAPDH expression ± SEM.

To assess the expression of the agrin gene in differentiated MNs, cDNA samples were prepared as mentioned above from 3 consecutive differentiations. Genes were amplified using Arktik thermal cycler according to the manufacturer's protocol (ThermoFisher). PCR amplification products were analyzed using 2% agarose gel electrophoresis and SYBR safe DNA gel stain

(Invitrogen). GAPDH gene expression was used as the loading control. The oligo sequences are summarized in **Table S3**.

Statistical Analysis

All experiments were performed using at least three different muscle cell lines derived from three separate patients (n = 3 biological replicates). Exceptions include Figure 1C and Figure 4D (n=1), and Figure 4J-L (n = 3 experimental replicates using one lentivirally transduced myogenic immortalized cell line and 3 different MG patient serum purified IgGs). Each experiment was performed at least in triplicate using each muscle cell line. For muscle / motor neuron co-cultures, each muscle cell line was co-cultured with at least one separate human pluripotent stem cell derived motor neuron population. Statistical analysis was performed using GraphPad Prism 6.0 software. Differences between experimental groups were determined by unpaired t-test or one-way ANOVA except for Figure 1B, where statistics were performed using two-way ANOVA followed by an unpaired t-test to determine the differences between data sets at each time point. Results are presented as mean ± SEM. $P < 0.05$ was considered significant for all statistical tests.

Acknowledgements

We would like to extend our thanks to Saint Michael's Hospital and Azienda Ospedaliera di Padova patients who agreed to contribute samples to our study. We would also like to thank the following sources for funding this study: Toronto Musculoskeletal Centre, Ontario Graduate Scholarship, and Krembil Foundation to M.A.B.; Postdoctoral NRSA from the NIH (1F32NS083291-01A1) to E.S.L.; TD Bank Health Research Fellowships at the LTRI (to B.M.); the Canadian Institute of Health Research and Natural Sciences and Engineering Research Council to (M.Z.); an Innovation in Regulatory Science Award for the Burroughs Wellcome Fund, NIH grant R21NS082618, and U.S. Environmental Protection Agency (EPA) Assistance Agreement No. 83573701 to R.S.A.; and Toronto Western Arthritis Program, Ontario Research Fund, Canada Research Chair's Program, Canada Foundation for Innovation, Canada First Research Excellence Fund 'Medicine by Design', and the University of Toronto Faculty of Medicine Deans Fund (to P.M.G.). We would also like to thank Dr. Majid Ebrahimi and Dr. Louise Moyle for reviewing the final manuscript and their critical feedback.

Author contributions

MAB designed and performed the experiments, analyzed and interpreted the data, and prepared the manuscript. ESL designed experiments, provided $OLIG2^+$ cells, provided training on differentiation of $OLIG2^+$ cells to motor neurons, interpreted the data, and revised the manuscript. BM designed and performed electrophysiological experiments, analyzed and interpreted the data, and prepared the manuscript. EP consented patients and collected sera from MG patients. KT consented patients, obtained research ethics board approval, and transferred tissue biopsies to MAB. HA and HG surgically resected and provided skeletal muscle biopsies, interpreted the data, and revised the manuscript. MZ designed experiments, interpreted data, and revised the manuscript. RSA designed experiments, interpreted data, and revised the manuscript. PMG designed the experiments, supervised the work, interpreted the data, prepared and revised the manuscript.

Competing financial interests.

The authors declare no competing financial interests.

Materials & Correspondence

Correspondence should be addressed to Penney M Gilbert.

Figure 1

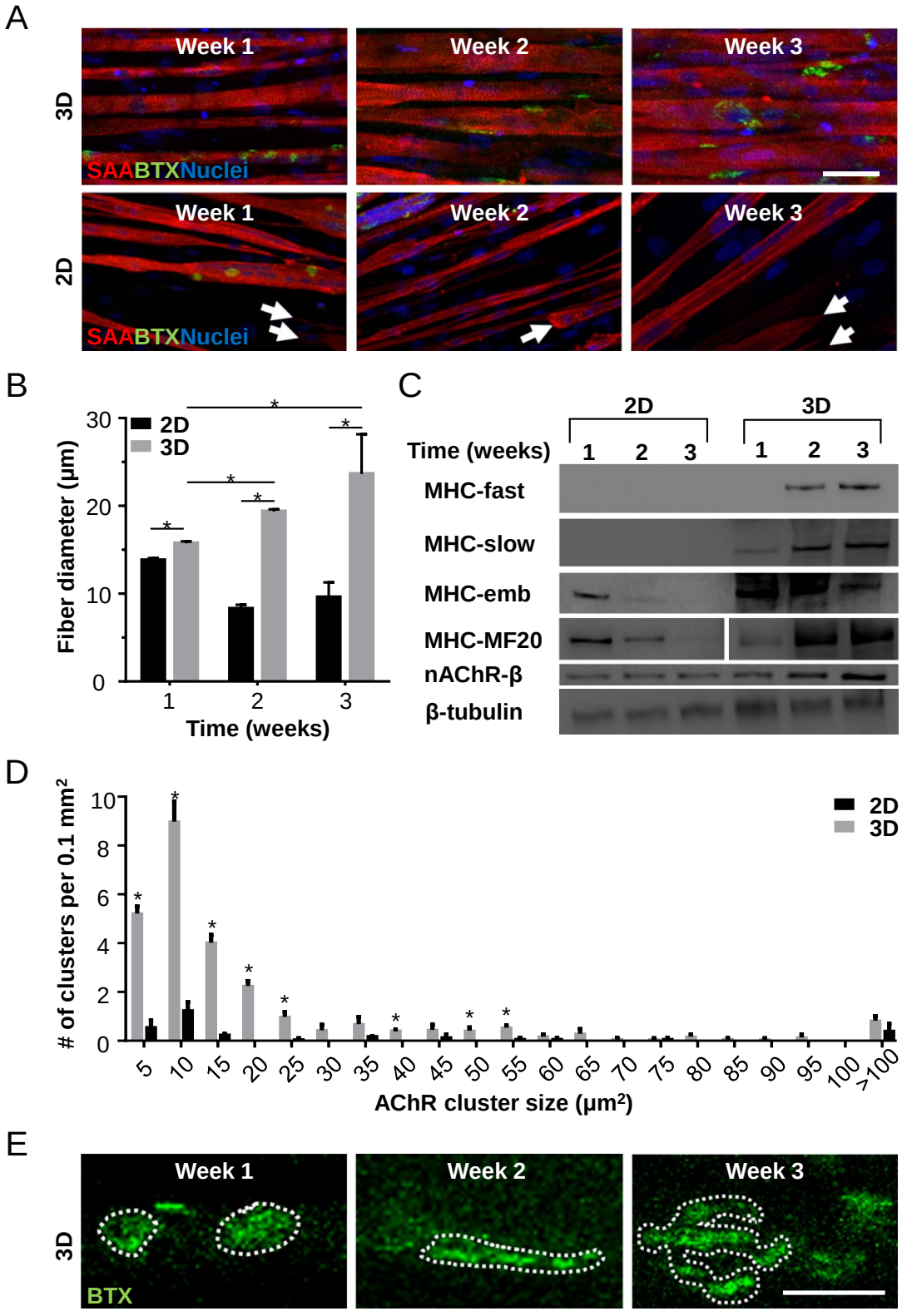

Figure 1. 3D culture enhances skeletal muscle fiber maturation over 2D culture.

(A) Representative confocal images of 3D muscle tissues and 2D muscle fibers immunostained for sarcomeric α-actinin (SAA; red), α-bungarotoxin (BTX; green), and Hoechst 33342 (blue) at 1, 2, and 3 weeks of culture. Scale bar, 50 μm. White arrowheads indicate broken fibers. **(B)** Bar graph of muscle fiber diameter quantified in 2D (black bars) and 3D (grey bars) cultures over time. **(C)** Western blot analysis of myosin heavy chain (MYH) isoforms (fast, slow, embryonic (emb), and pan (MF-20)) and nicotinic AChRβ (nAChRβ) in 2D compared with 3D cultures over time. **(D)** Histogram of AChR cluster number per 0.1 mm^2 observed in 2D muscle fibers (black bars) and 3D muscle tissue (grey bars) cultures at two weeks of culture. **(E)** Representative confocal images of BTX-labeled AChR clusters observed in 3D muscle cultures at 1, 2, and 3 weeks of culture. Scale bar, 25 μm.

Figure 2

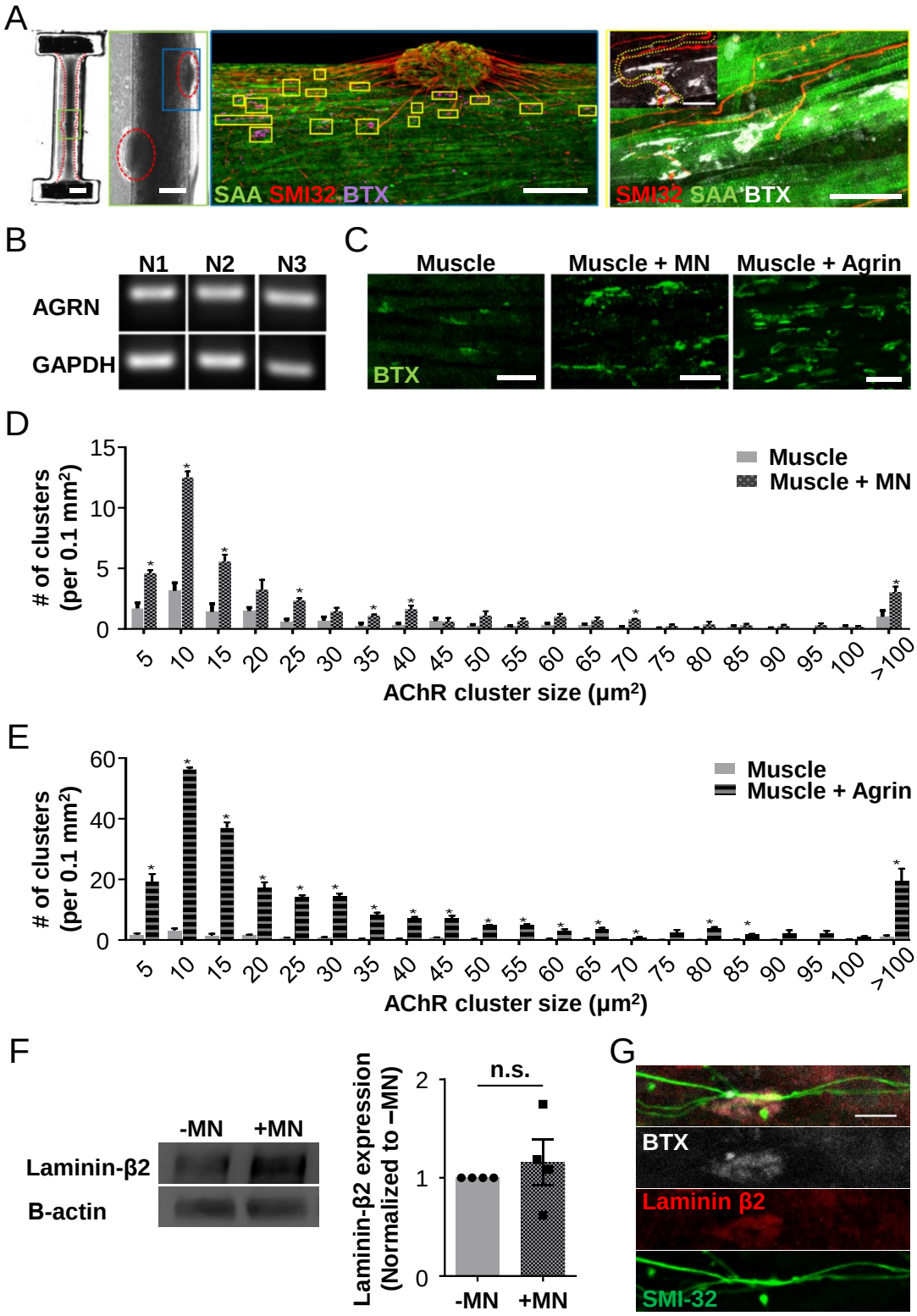

Figure 2. 3D neuromuscular co-culture augments AChRs clustering via secreted motor neuron trophic factors. (A) Left panel: Stitched phase contrast image of a representative 3D skeletal muscle-motor neuron (MN) co-culture at two weeks of culture. Neuromuscular tissue outlined with red dashed line. Region outlined in green box is magnified in the image to the right. Red dashed lines in right panel outline motor neuron clusters. Scale bars, 2 mm and 200 μm on the left and right panels respectively**. Middle panel:** Representative confocal image of a two-week old neuromuscular co-culture immunostained for sarcomeric α-actinin (SAA; green), α-bungarotoxin (BTX; magenta), and neurofilament heavy SMI-32 (red). AChR clusters are outlined with yellow boxes. Scale bar, 200 μm. **Right panel:** Representative confocal image indicating co-localization of a SMI-32 (red) labeled neurite terminal and a BTX labelled AChR cluster on a striated muscle fiber as seen by SAA (green) staining. Scale bar, 50 μm. **(B)** PCR agarose gel bands of agrin (AGRN) and GAPDH gene expression in three independent pluripotent stem cell derived motor neuron differentiations. **(C)** Representative confocal image of BTX labelled AChR clusters in 3D muscle alone (left), 3D neuromuscular (middle), and agrin treated (right) 3D muscle cultures. Scale bar, 50 μm. **(D-E)** Histograms of AChR cluster number per 0.1 mm^2 in **(D)** muscle alone (grey bars) and 3D neuromuscular cultures (black bars) or **(E)** 3D muscle tissues treated with agrin (striped) and analyzed after two weeks of culture. **(F)** Representative western blot (left) and bar graph (right) showing quantification of laminin-β2 in 3D muscle and neuromuscular co-cultures at two weeks. **(G)** Representative confocal image of a neuromuscular co-culture immunostained for the basement membrane protein laminin-β2 (red), AChRs (BTX, white), and MN neurites (SMI-32, green). Scale bar, 10 μm.

Figure 3

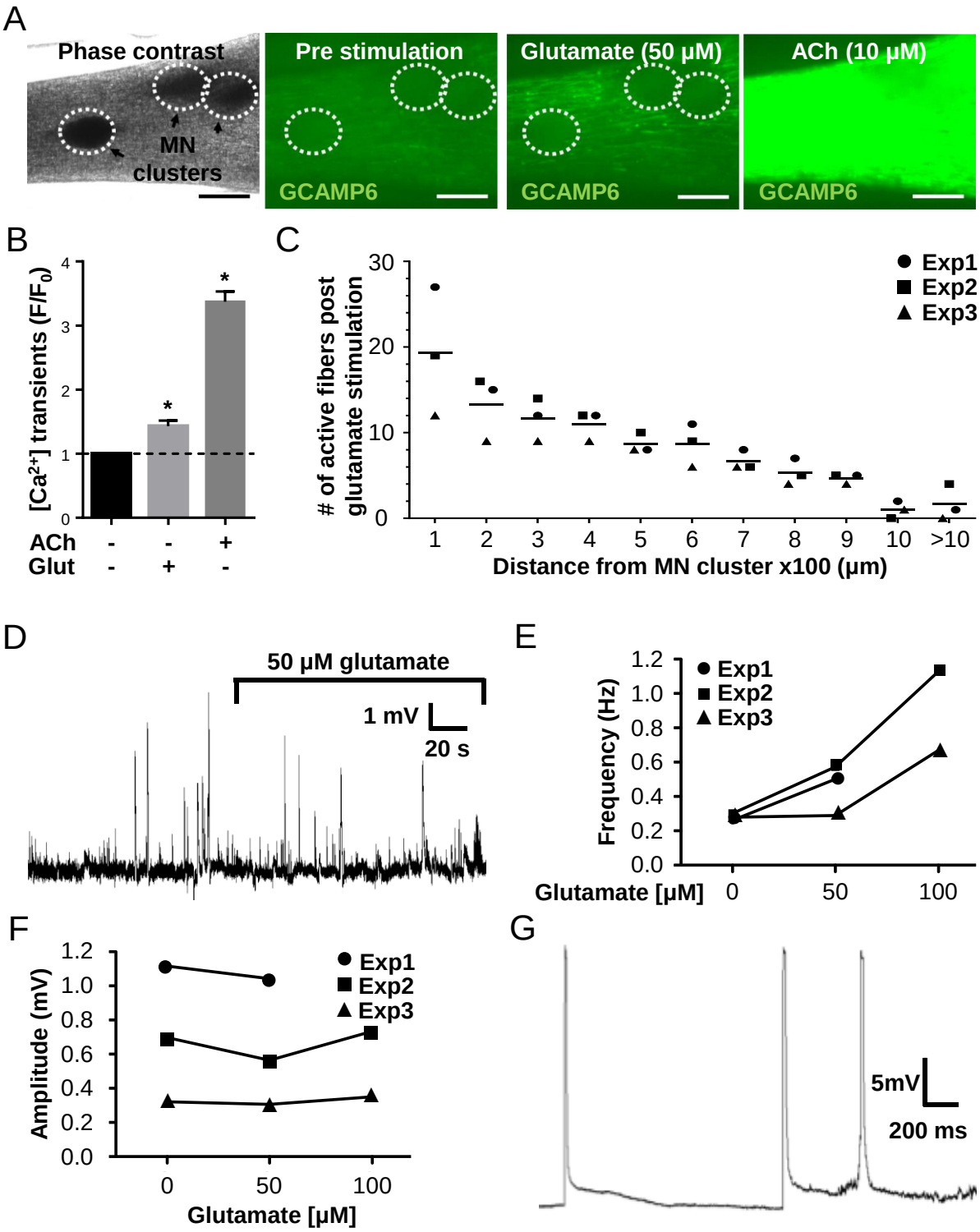

Figure 3. 3D neuromuscular co-cultures are functionally innervated.

(A) Phase contrast (far left panel) and GCaMP6 epifluorescence images (right panels) of a 3D neuromuscular co-culture after treatment with phosphate buffered saline (middle left panel), glutamate (middle right panel), or ACh (far right panel). Motor neuron clusters are outlined with white dashed lines. Scale bar, 250 μm. **(B)** Bar graph indicating quantification of fluorescence signal from neuromuscular co-cultures following glutamate and ACh stimulation relative to treatment with phosphate buffered saline. **(C)** Histogram indicating the number of functionally innervated fibers relative to distance from the motor neuron cluster in three independent experiments at two weeks of culture. **(D)** Representative trace of a sharp microelectrode recording showing mEPPs in a neuromuscular co-culture before and after addition of 50 μM glutamate to the bath media. **(E-F)** Graphs indicating the frequency **(E)** and amplitude **(F)** of mEPPs in three independent 3D neuromuscular cultures, in response to treatment with increasing concentration of glutamate. **(G)** Representative action potential-like events recorded from a 3D neuromuscular co-culture following glutamate stimulation.

Figure 4

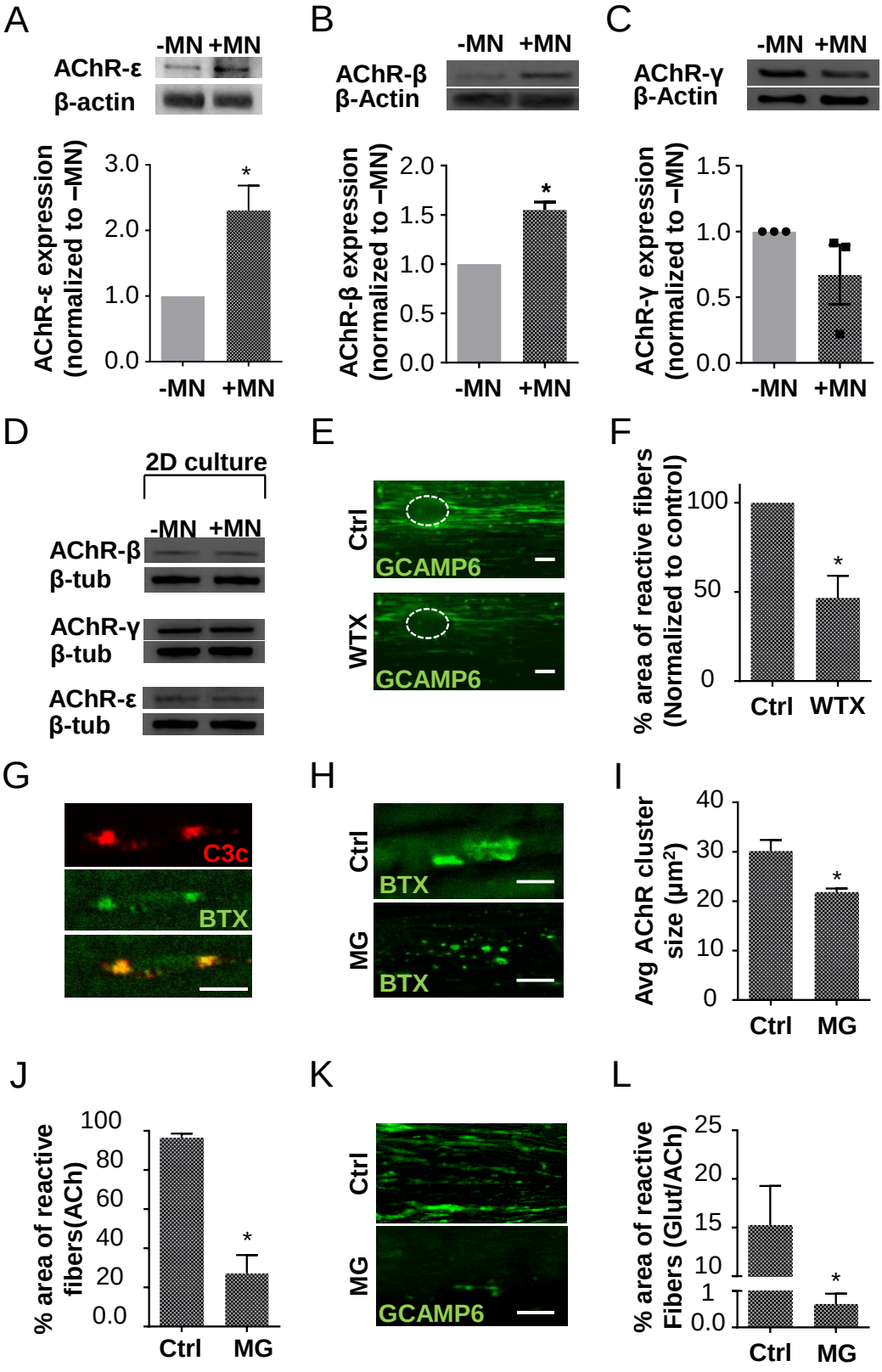

Figure 4. Pharmacological validation of adult NMJ function in 3D neuromuscular co-cultures. (A-C) Representative western blot image and bar graph quantification of nicotinic acetylcholine receptor subunit **(A)** epsilon (nAChR-ε), **(B)** beta (nAChR-β), and **(C)** gamma (nAChR-γ) protein expression in 3D muscle cultures (-MN) and 3D neuromuscular co-cultures (+MN) at day 14 of culture. **(D)** Representative western blot images of nicotinic acetylcholine receptor subunit beta, gamma, and epsilon subunit protein expression in 2D muscle fiber (-MN) and neuromuscular co-cultures (+MN) at two weeks of culture. **(E)** Representative epifluorescence images of GCaMP6 signals from a 3D neuromuscular co-culture responding to glutamate stimulation before (top panel; Ctrl) and after (bottom panel) treatment with Waglerin-1 (WTX). Scale bar 100 μm. **(F)** Bar graph quantifying the percent area of reactive fibers ($GCaMP6^{+}$) within 3D neuromuscular co-cultures stimulated with glutamate before and after WTX (1μM) treatment. Data normalized to control (Ctrl). **(G)** Representative confocal images of a 3D muscle culture treated with Myasthenia gravis patient IgG and human complement and then stained for human complement component C3c (red, top) and bungarotoxin (BTX, green, middle) to visualize AChR clusters. Bottom panel is a merged image of the top and middle panels. Scale bar, 10 μm. **(H)** Representative confocal images of 3D muscle cultures treated with healthy (Ctrl) or Myasthenia gravis (MG) patient IgG in the presence of human complement for 72 hours and then immunostained with bungarotoxin (BTX, green). Scale bar, 20 μm. **(I)** Bar graph indicating average AChR cluster size quantified from healthy (Ctrl) and MG patient IgG treated muscle cultures. **(J)** Bar graph indicating the percent area occupied by fibers responding to acetylcholine (ACh) stimulation in healthy (Ctrl) and MG patient IgG treated neuromuscular co-cultures. Data reported as percent total tissue area. **(K)** Representative epifluorescence images of GCaMP6 signals from a 3D neuromuscular co-culture responding to glutamate stimulation

following a 72-hour treatment with 300 nM of healthy (Ctrl, top panel) or MG (bottom panel) patient IgG and human complement. Scale bar 100 μm. **(L)** Bar graph indicating the percent area occupied by fibers responding to glutamate (glut, 50 μM) stimulation in healthy (Ctrl) and MG patient IgG treated neuromuscular co-cultures. Data normalized to the total area fibers in each tissue that reacted to ACh stimulation by producing a GCaMP6 signal.

Supplemental Information

A 3D model of human skeletal muscle innervated with stem cell-derived motor neurons enables epsilon-subunit targeted myasthenic syndrome studies

Mohsen Afshar Bakooshli, Ethan S Lippmann, Ben Mulcahy, Kayee Tung, Elena Pegoraro, Henry Ahn, Howard Ginsberg, Mei Zhen, Randolph S Ashton, Penney M Gilbert

Supplemental Figure 1

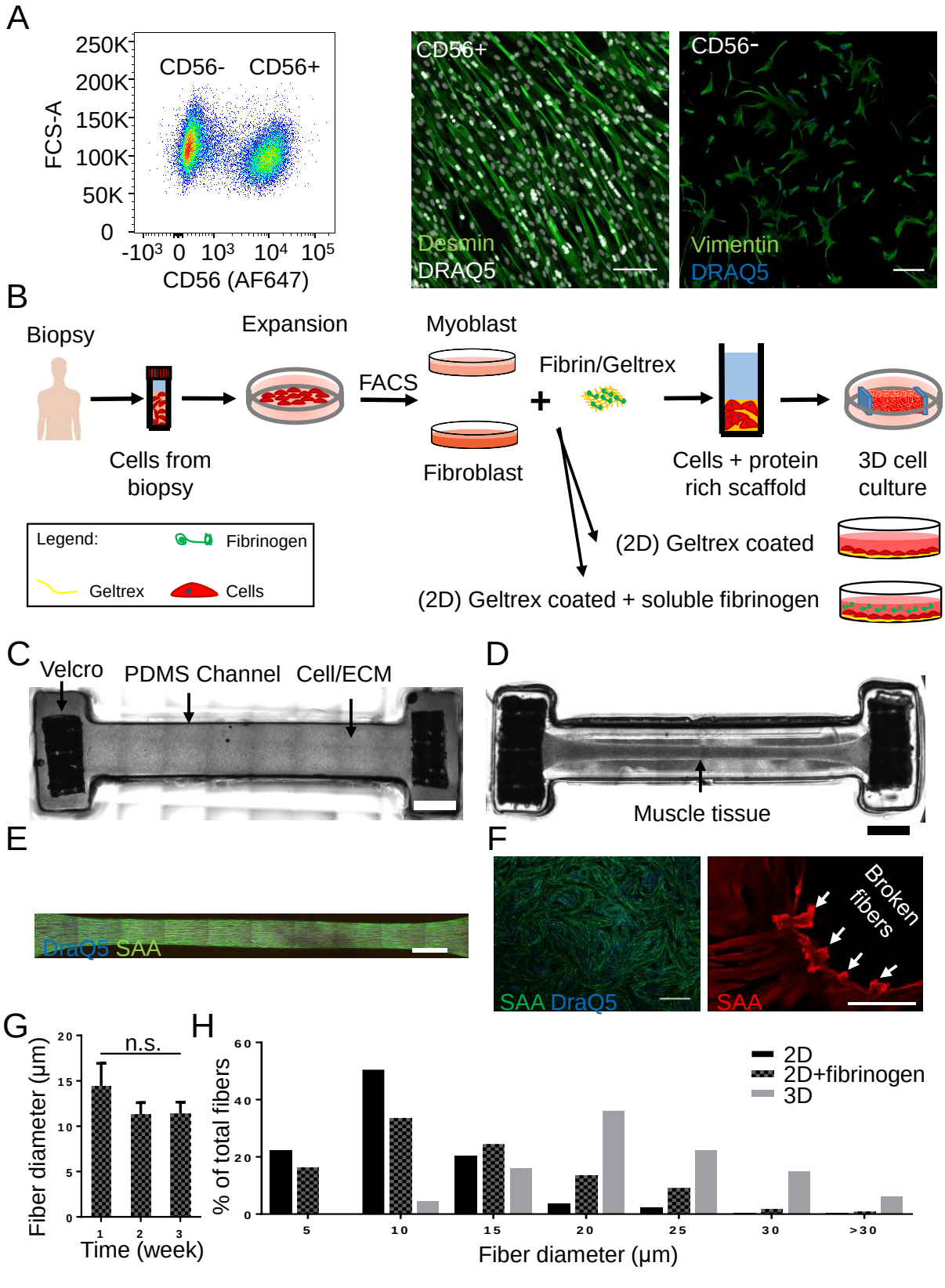

Figure S1 (Related to Figure 1). Generation of two- and three-dimensional culture models of human muscle fibers. (A) Left panel: Representative flow plot of fluorescence activated cell sorted (FACS) human myoblasts ($CD56^{+}$) and fibroblasts ($CD56^{-}$). **Middle panel:** Representative confocal image of 2D muscle fiber culture established from the $CD56^{+}$ population and immunostained for desmin (green) and DRAQ5 (white) to visualize the nucleus. **Right panel:** Representative confocal image of $CD56^{-}$ population in 2D culture immunostained for vimentin (green) and DRAQ5 (blue). Scale bars, 100 μm left panel and 200 μm right panel. **(B)** Schematic overview of human muscle cell isolation and downstream culture methods. **(C-D)** Stitched phase contrast tiled image of a representative well **(C)** immediately after seeding the muscle cell / extracellular matrix scaffold mix into the PDMS channel and **(D)** after two weeks of differentiation. Scale bar, 2 mm. Black arrows indicate the location of the PDMS channel, the Velcro™ attachments, and the forming muscle tissue. Scale bar, 2 mm. **(E)** Confocal tiled and stitched immunofluorescence image of a representative 3D skeletal muscle tissue immunostained for sarcomeric α-actinin (green) and DRAQ5 (blue). **(F) Left panel:** 2D muscle fiber culture after two weeks of differentiation immunostained for sarcomeric α-actinin (green), α-bungarotoxin (red) and DRAQ5 (blue). Scale bar, 1 mm. **Right panel:** Magnified confocal image of a 2D muscle culture at two weeks of differentiation immunostained for sarcomeric α-actinin (red). White arrowheads indicate broken fibers. Scale bar, 100 μm. **(G)** Bar graph indicating average muscle fiber diameter quantified from 2D fibrinogen/Geltrex™ muscle fiber cultures over time. **(H)** Histogram displaying muscle fiber diameter quantified from 2D Geltrex™ (black bars), 2D fibrinogen/Geltrex™ (patterned bars), and 3D fibrin/Geltrex™ (grey bars) muscle fiber culture conditions.

Supplemental Figure 2

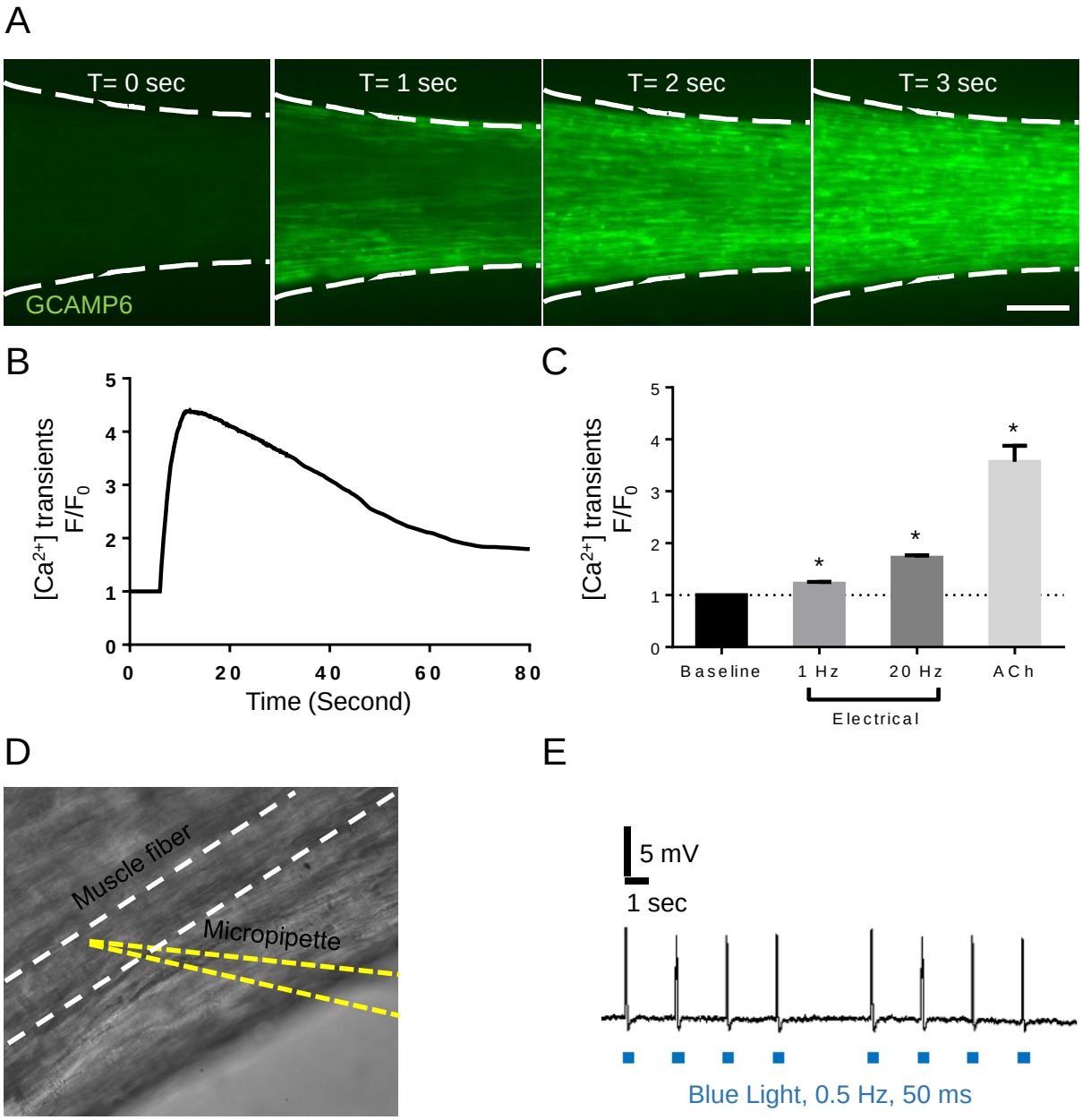

Figure S2 (Related to Figure 1). Functional characterization of 3D skeletal muscle tissues.

(A) Representative epifluorescence images of a GCaMP6 transduced 3D muscle tissue indicating the calcium transients of muscle fibers at time-points before and after ACh stimulation. Scale bar, 250 μm. **(B)** Graph quantifying a time course of GCaMP6 reporter fluorescence following ACh-induced stimulation of a 3D muscle tissue. **(C)** Bar graph showing quantification of

GCaMP6 signal after exposing 3D skeletal muscle tissues to low (1Hz) or high (20Hz) electrical stimulation or ACh biochemical stimulation relative to phosphate buffered saline treated control tissues (baseline). **(D)** Representative bright-field image of the sharp microelectrode recording of a muscle fiber within a 3D human skeletal muscle tissue. Micropipette is outlined with a yellow dashed line and the muscle fiber is outlined with white dashed lines. **(E)** Representative sharp microelectrode recording of a ChR2 transduced 3D muscle tissue after two weeks of culture. Blue light stimulation points are indicated by blue squares under the trace.

Supplemental Figure 3

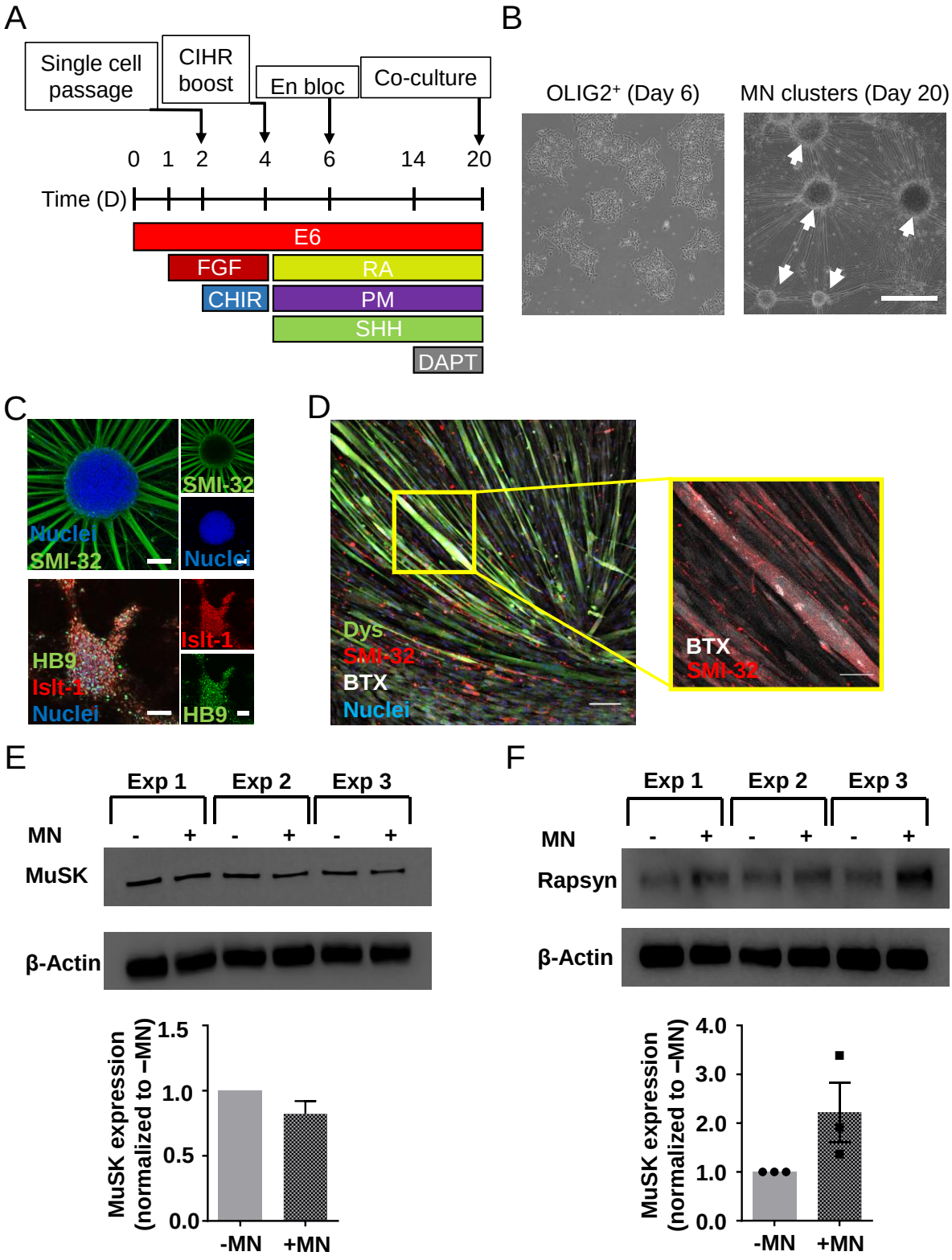

Figure S3 (Related to Figure 2). Differentiation and characterization of post-mitotic motor neurons derived from human ESCs. (A) Schematic diagram of the protocol and timeline for differentiation of OLIG2^{+} progenitors to a post-mitotic motor neuron (MN) fate. **(B)** Representative bright field images of the OLIG2^{+} (left panel) progenitors after 6 days of differentiation and post-mitotic MN cluster (right panel) after 20 days of differentiation. White arrows point to motor neuron clusters. Scale bar, 500 μm. **(C) Top panels:** Merged (left) and split (right) representative confocal image of a day 20 motor neuron cluster immunostained for the neurofilament heavy chain SMI-32 (green; and top right image) and Hoechst 33342 (blue; and bottom right image). Scale bars, 100 μm. **Bottom panels:** Merged (left) and split (right) representative confocal image of a day 20 MN cluster immunostained for the ISL1 (red; and top right image) and HB9 (green; and bottom right image) transcription factors and Hoechst 33342 (blue). Scale bars, 100 μm. **(D)** Representative confocal images of 2D neuromuscular co-cultures immunostained for dystrophin (green), neurofilament heavy SMI-32 (red), α-bungarotoxin (BTX, white), and Hoechst 33342 (blue) on the second week of culture. Scale bar, 100 μm. Inset scale bar, 50 μm. **(E-F)** Western blots (top) and bar graph (bottom) showing quantification of **(E)** muscle specific kinase (MuSk) and (F) rapsyn protein in 3D muscle (-MN) and neuromuscular co-cultures (+MN) at two weeks of culture. Muscle tissues established from muscle cell lines derived from three patients and co-cultured with three separate pluripotent stem cell MN differentiations is shown.

Supplemental Figure 4

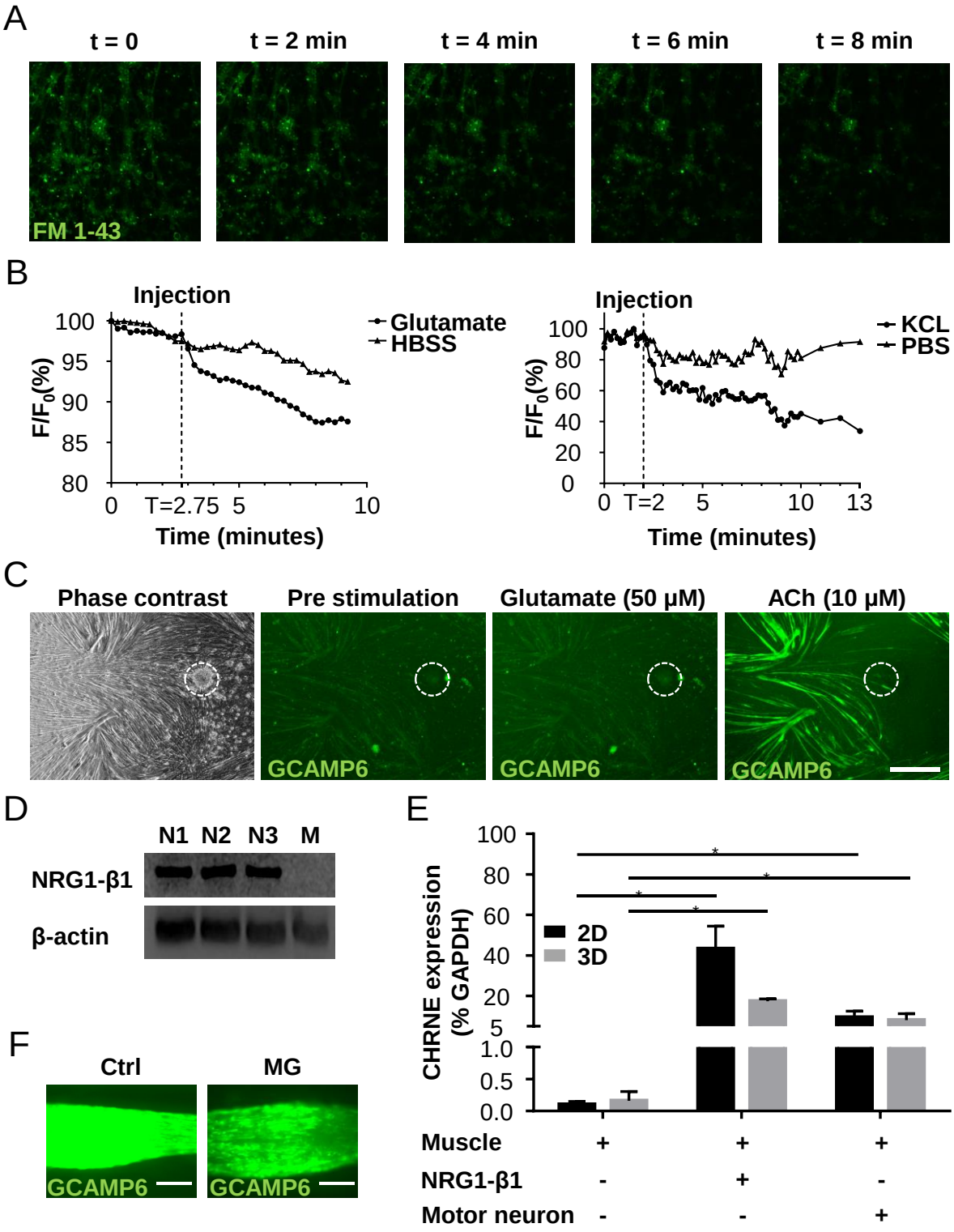

Figure S4 (Related to Figure 3 (A-C) and Figure 4 (A-F)). Functional characterization of 2D motor neuron cultures and neuromuscular co-cultures. (A) Representative epifluorescence images and **(B)** graphs quantifying a time course of fluorescence intensity during a potassium chloride **(A** and **B, left panel)** or glutamate **(B, right panel)** stimulation of differentiated MN cultures loaded with styryl dye FM 1-43 as compared to phosphate buffered saline or Hank's buffered salt solution as carrier control treatments. **(C)** Phase contrast (far left panel) and GCaMP6 epifluorescence images of a 2D neuromuscular co-culture after treatment with phosphate buffered saline (middle left panel, pre-stimulation), glutamate (middle right panel), or ACh (far right panel). Motor neuron cluster is outlined with white dashed lines. Scale bar, 250 μm. **(D)** Western blot analysis of neuregulin 1-β1 (NRG1- β1; top image) and β-actin (bottom image) protein expression in three independent pluripotent stem cell derived motor neuron cultures (N1 – N3) compared to a 3D muscle control (M). **(E)** Bar graph of qRT-PCR quantification of epsilon subunit of AChR (CHRNE) gene expression in 2D (black bars) and 3D (grey bars) muscle alone, NRG1- β1 treated, and neuromuscular co-cultures. **(F)** GCaMP6 epifluorscence images of 3D neuromuscular co-cultures treated with control (Ctrl, left) or myasthenia gravis (MG, right) patient IgG and human complement after ACh (100 μM) stimulation. Scale bars, 250 μm.

Table S1. List of primary antibodies

#	Antibody	Species	Dilution	Source
1	Alexa Fluor 647 mouse anti-human CD56	Mouse	1:20	BD Pharmingen
2	Anti-200 kD neurofilament heavy (SMI-32)	Rabbit	1:200	Abcam
3	Anti-C3c (FITC)	Rabbit	1:200	Abcam
4	Anti-HB9/HLXB9	Rabbit	1:100	Abcam
5	Anti-vimentin	Rabbit	1:100	Abcam
6	Anti- β -tubulin	Rabbit	1:5000	Cell Signaling
7	DRAQ5	-	1:1000	ThermoFisher
8	Hoechst 33342	-	1:1000	ThermoFisher
9	Islet-1	Goat	5 μg/ml	R&D systems
10	NRG1- β1	Mouse	1:500	R&D Systems
11	Monoclonal anti-β-actin-peroxidase	Mouse	1:50000	Sigma
12	Monoclonal mouse anti-human desmin	Mouse	1:100	Dako
13	MuSK	Rabbit	1:1000	Invitrogen
14	Myosin heavy chain - embryonic	Mouse	1:50	DSHB
15	Myosin heavy chain - fast	Mouse	1:50	DSHB
16	Myosin heavy chain - slow	Mouse	1:50	DSHB

17	Myosin heavy chain - pan	Mouse	1:50	DSHB
18	Nicotinic acetylcholine receptor β	Rabbit	1:2000	Novus
19	Nicotinic acetylcholine receptor epsilon	Rabbit	1:1000	Novus
20	Rapsyn	Mouse	1:1000	Abcam
21	Sarcomeric alpha-actinin	Mouse	1:200	Sigma
22	α-Bungarotoxin, Alexa Fluor 647 conjugate	-	1:500	ThermoFisher

Table S2. Cell Culture Media and Solutions

#	Name	Details
1	Blocking solution	20% goat serum, 0.3% Triton-X 100 in PBS
2	Fibrinogen stock solution	10 mg/ml fibrinogen in 0.9% (wt/v) NaCl solution in water
3	Human fibroblast growth media	Dulbecco's Modified Eagle's medium (DMEM), 10% fetal bovine serum, 1% penicillin-streptomycin
4	Human myoblast differentiation media	Dulbecco's Modified Eagle's medium (DMEM), 2% horse serum, 10 µg/ml insulin, 1% penicillin-streptomycin
5	Human myoblast growth media	Ham's F-10 nutrient mix, 20%v fetal bovine serum, 5 ng/ml basic fibroblast growth factor, 1% penicillin-streptomycin
6	Hydrogel mixture	Dulbecco's Modified Eagle's medium (DMEM), 4 mg/ml bovine fibrinogen, Geltrex (20% v/v), thrombin (0.2 unit/mg fibrinogen)
7	Milk based blocking solution	5% (wt/v) skim milk (BioShop) in TBST
8	Red blood cell lysis buffer	15.5 mM NH4Cl, 1 mM KHCO3, 10 µM EDTA
9	Tris-buffered saline Tween (TBST)	50 mM Tris (BioShop), 150 mM NaCl (Sigma), 0.1% (v/v) Tween 20 (BioShop)

Table S3. Real-time PCR primer sequences

GENE	Species	Forward 5'-3'	Reverse 3'-5'
AGRN	human	CCTGACCCTCAGCTGGCCCT	AGATACCCAGGCAGGCGGCA
GAPDH	human	GTGAAGGTCGGAGTCAACG	TGAGGTCAATGAAGGGGTC

Table S4. Myasthenia Gravis patient information

Patient ID	Sex	Anti-AChR titer (nM)
MG#1	Male	>10
MG#2	Female	8.6
MG#3	Female	>10

Supplementary Movie Captions

Movie S1. Three-dimensional human skeletal muscle tissue contraction in response to chemical and electrical stimulation. A series of four representative bright-field real-time videos of three-dimensional human muscle tissues after 10-12 days of culture exhibiting spontaneous contractions, or contracting in response to electrical (1Hz, 20Hz) or acetylcholine (10 μM) stimulation.

Movie S2. Two-dimensional human skeletal muscle tissue contraction in response to acetylcholine stimulation. Epifluorescence real-time video of two-dimensional GCaMP6 transduced human muscle fiber culture contraction in response to 10 μM acetylcholine stimulation after 2-weeks of culture. Red arrow heads indicate a muscle fiber that breaks post acetylcholine stimulation.

Movie S3. Three-dimensional human skeletal muscle tissue calcium handling in response to chemical stimulation. A series of two representative epifluorescence time-lapse videos of three-dimensional human skeletal muscle tissues after 10-12 days of culture stimulated with acetylcholine (10 μM) and L-glutamate (50 μM). Muscle fiber calcium transients are visualized in green by following a GCaMP6 calcium reporter that was transduced into the human muscle cells.

Movie S4. Optogenetically transduced three-dimensional human skeletal muscle tissue response to blue light (470 nm). A real-time bright field movie of a 3D human skeletal muscle

tissue transduced with ChR2 (H134R) and stimulated by blue light. Red circles indicate the time and period of light pulses.

Movie S5. Pluripotent stem cell derived motor neurons exocytose in response to physiological stimuli. A representative time-lapse microscope videos depicting exocytosis induced in pluripotent stem cell derived motor neuron clusters by stimulating with KCl (60 mM).

Movie S6. Neuromuscular co-cultures are functionally innervated. A representative epifluorescence time-lapse video in which GCaMP6 transduced muscle cells co-cultured with pluripotent stem cell-derived motor neurons for 14 days in three-dimensions are then treated with HBSS saline solution, followed by L-glutamate (50 μM), and then acetylcholine (10 μM). White dashed lines outline the muscle tissue and yellow dotted circles outline motor neuron clusters.

Movie S7. 2D neuromuscular co-culture innervation and AChR development is limited. A representative epifluorescence time-lapse videos in which GCaMP6 transduced muscle cells co-cultured with pluripotent stem cell-derived motor neurons for two-weeks in 2D culture are treated with L-glutamate (50 μM) on Day 14, with Waglerin-1 (WTX) followed by L-glutamate on Day 15, and then with acetylcholine (10 μM). Muscle fiber calcium transients are visualized in green by following the GCaMP6 calcium reporter.

Movie S8. 3D neuromuscular co-cultures enable studies of the AChR epsilon subunit. A representative epifluorescence time-lapse video in which GCaMP6 transduced muscle cells co-cultured with pluripotent stem cell-derived motor neurons for two-weeks in 3D culture are

treated with L-glutamate (50 μM) on Day 14, and then with Waglerin-1 (WTX) followed by L-glutamate (50 μM) on Day 15. Muscle fiber calcium transients are visualized in green by following the GCaMP6 calcium reporter. A yellow dotted line outlines the location of the motor neuron cluster.

Movie S9. Waglerin-1 treatment does not affect muscle fiber calcium transients in 3D muscle alone cultures post ACh stimulation. A representative epifluorescence time-lapse video in which GCaMP6 transduced muscle cells cultured two-weeks in 3D culture are treated with ACh (10 μM) on Day 14, and then with Waglerin-1 (WTX, 1 μM) followed by ACh (10 μM). Muscle fiber calcium transients are visualized in green by following the GCaMP6 calcium reporter.

Movie S10. 3D neuromuscular co-cultures treated with healthy patient IgG and complement exhibit robust calcium transients in response to glutamate stimulation. A representative epifluorescence time-lapse video in which GCaMP6 transduced muscle cells co-cultured with pluripotent stem cell-derived motor neurons for 14 days in three-dimensions are stimulated with L-glutamate (50 μM), and then acetylcholine (100 μM). Cultures were treated for 3 days (Day 11 to Day 14) with healthy patient IgG (300 nM) and 2% human serum. A yellow dotted line outlines the location of the motor neuron cluster.

Movie S11. 3D neuromuscular co-cultures are an ideal system to study the influence of Myasthenia gravis autoantibodies on NMJ activity. A representative epifluorescence time-lapse video in which GCaMP6 transduced muscle cells co-cultured with pluripotent stem cell-

derived motor neurons for 14 days in three-dimensions are stimulated with L-glutamate (50 μM), and then acetylcholine (100 μM). Cultures were treated for 3 days (Day 11 to Day 14) with Myasthenia gravis patient IgG (300 nM) and 2% human serum. A yellow dotted line outlines the location of the motor neuron cluster.